Intermediate Flortaucipir uptake is associated with amyloid-β PET & cerebrospinal fluid tau in cognitively normal older adults

Melissa McSweeney

Integrated Program in Neuroscience, McGill University, Montreal

August 2019

A thesis submitted to McGill University in partial fulfillment of the requirements of the degree of Master of Science

Table of Contents

Abstract: English

Hyperphosphorylated tau protein in the form of neurofibrillary tangles is one of the major pathological hallmarks of Alzheimer's disease (AD). This thesis explores early tau accumulation, as measured with the positron emission tomography (PET) imaging radiotracer [^{18}F]flortaucipir, and its associations with Alzheimer's disease-related biological and cognitive markers in cognitively intact older adults with a familial history of sporadic Alzheimer's disease. We show that flortaucipir binding in cognitively normal older adults is associated with three key markers of Alzheimer's disease: amyloid-beta PET tracer retention, phosphorylated tau in the cerebrospinal fluid, and cognitive performance. Moreover, the associations of flortaucipir with Aβ and cerebrospinal fluid phosphorylated tau are evident at subthreshold levels of flortaucipir binding. These results suggest that intermediate levels of flortaucipir retention can indicate meaningful pathological changes associated with Alzheimer's disease before the onset of clinical symptoms, while higher levels of flortaucipir retention may be necessary to observe associations with worse cognitive performance on a group level.

Le Résumé: Français

Les enchevêtrements neurofibrillaires composés de protéines tau hyperphosphorylées sont l'un des principaux signes pathologiques de la maladie d'Alzheimer (MA). Cette thèse explore l'accumulation précoce de tau, mesurée en tomographie par émission de positrons (TEP) à l'aide du radiotraceur [^{18}F]flortaucipir, et ses associations avec les marqueurs biologiques et cognitifs liés à la maladie d'Alzheimer chez des personnes âgées sans trouble cognitif avec antécédents familiaux de la forme sporadique de la MA. Nous montrons que la rétention du traceur flortaucipir chez les personnes âgées cognitivement normales est associée à trois marqueurs clés de la MA: la rétention du traceur bêta-amyloïde (Aβ) TEP, la tau phosphorylée dans le liquide cérébro-spinal et les performances cognitives. De plus, les associations de flortaucipir avec Aβ et la protéine tau phosphorylée dans le liquide cérébro-spinal sont évidentes même à des niveaux faibles de rétention du flortaucipir. Ces résultats suggèrent que même de faibles quantités de rétention du flortaucipir peuvent indiquer des modifications pathologiques significatives associées à la MA avant l'apparition de symptômes cliniques. En revanche, des quantités plus élevées de rétention du flortaucipir sont nécessaires pour observer des associations avec des performances cognitives.

List of Abbreviations

Aβ= amyloid-beta; **AD**=Alzheimer's disease; **APOE**=Apolipoprotein E, **CDR**=Clinical Dementia Rating; **CSF**= Cerebrospinal fluid, **FDR**=False discovery rate; FTP=[^{18}F]Flortaucipir; **GMM**=Gaussian mixture modeling, **MCI**=Mild cognitive impairment; **MMSE**= Mini Mental State Exam; **MRI**=Magnetic resonance imaging, **NAV**=[^{18}F]NAV4694; **p-tau**= phosphorylated tau; **PET**= Positron emission tomography, **PREVENT-AD**= PResymptomatic EValuation of Experimental and Novel Treatment of Alzheimer's disease, **RBANS**= Repeatable Battery for the Assessment of Neuropsychological Status; **ROI**=Region of interest; **spEYO**=years to estimated symptom onset (sporadic Alzheimer's disease), **SUV**=Standardized uptake ratio, **SUVR**= Standardized uptake value ratio

List of Figures

List of Tables

Acknowledgments

Contributions of co-authors to submitted manuscript included in this thesis

Name	Location	Role	Contribution
Melissa McSweeney	McGill University, Montreal, Quebec, Canada	Co-first Author	Study concept and design, data acquisition, statistical analysis and interpretation of data, drafting the manuscript for intellectual content.
Alexa Pichet Binette, MSc	McGill University, Montreal, Quebec, Canada	Co-first Author	Advice on study concept and design, data acquisition, advice on interpretation of data, revising the manuscript for intellectual content. Co-first author credit; permission for inclusion in thesis provided.
Pierre-François Meyer, MSc	McGill University, Montreal, Quebec, Canada	Author	Mentorship in statistical programming in R, revising the manuscript for intellectual content
Julie Gonneaud, PhD	McGill University, Montreal, Quebec, Canada	Author	Mentorship in PET imaging, data acquisition, revising the manuscript for intellectual content
Christophe Bedetti, MSc	McGill University, Montreal, Quebec, Canada	Author	Computational processing of imaging data
Hazal Ozlen, BSc	McGill University, Montreal, Quebec, Canada	Author	Data acquisition
Anne Labonté, BSc	McGill University, Montreal, Quebec, Canada	Author	Laboratory analysis of CSF data
Pedro Rosa-Neto, MD, PhD	McGill University, Montreal, Quebec, Canada	Author	Acquisition of data, revising the manuscript for intellectual content
John Breitner, MD	McGill University, Montreal, Quebec, Canada	Author	Acquisition of data, protocol concept and design, revising the manuscript for intellectual content
Judes Poirier, PhD	McGill University, Montreal, Quebec, Canada	Author	Acquisition of data, protocol concept and design, revising the manuscript for intellectual content
Sylvia Villeneuve, PhD	McGill University, Montreal, Quebec, Canada	Author	Principal Investigator, acquisition of data, study concept and design, interpretation of data, revision of manuscript for intellectual content

We also wish to acknowledge the PREVENT-AD staff, especially Jennifer Tremblay-Mercier and Leslie-Ann Daoust, as well as Dr. Theresa Köbe, the Brain Imaging Center of the Douglas Mental Health Research Institute and the PET and cyclotron units of the Montreal Neurological Institute. A full listing of the PREVENT-AD Research Group members can be found at https://preventad.loris.ca/acknowledgements/acknowledgements.php?date=[2018-11-14]. We would also like to acknowledge the participants of the PREVENT-AD cohort for dedicating their time and energy to helping us collect these data.

Thesis Format: Manuscript-based Thesis

This thesis is centered around a manuscript that was submitted for publication in March 2019 and resubmitted after major revisions in August 2019. The co-authors have provided their consent for the inclusion of this manuscript in my thesis. The co-first author of the manuscript, Alexa Pichet Binette, has provided further written consent that she will not include the contents of this manuscript in her PhD thesis.

In select sections of the introductory chapter, I have also included quotes from a published book chapter I co-authored earlier this year. [1]. I have formatted quotes from this book chapter according to McGill University's thesis guidelines. None of the quoted material overlaps with material in another student's thesis. I have submitted permissions requests to the publishing company, Elsevier, for use of this material in my thesis, and their permissions policies allow the reuse of published materials within student theses and dissertations.

CHAPTER I:

Introduction to Preclinical Alzheimer's disease, biomarkers, and PET imaging

Background Information

The Alzheimer's Continuum and Preclinical AD

Alzheimer's disease (AD) starts well before the onset of dementia [2]. Abnormal expression of biomarkers associated with late-onset sporadic Alzheimer's disease (AD) can begin decades before the onset of symptoms. According to the amyloid cascade hypothesis, changes in levels of beta-amyloid$_{1\text{-}42}$ (Aβ_{42}) in the cerebrospinal fluid (CSF) and Aβ plaques in the brain are the first signs of AD pathology, followed by an increase in phosphorylated (p)-tau in the CSF and brain and subsequent neurodegeneration [3]. These molecular processes lead to the hallmark AD symptoms of cognitive decline and, eventually, impairment in activities of daily living.

According to the new National Institute on Aging and Alzheimer's Association (NIA-AA) research framework, AD should be classified and diagnosed on a continuum based on the progression of these markers [4]. When these molecular changes are accompanied by abnormal cognitive decline, one can be diagnosed with mild cognitive impairment caused by AD. The onset of dementia and notable functional impairment in addition to the previous indicators would classify a diagnosis of AD dementia. Within this framework, individuals who have abnormal biomarker expression (namely those classified as amyloid positive based on Aβ PET and/or CSF results) while remaining cognitively unimpaired are classified as having a preclinical pathological change or preclinical AD. Identifying individuals within this preclinical phase of the AD continuum is important, as such individuals may be most likely to benefit from preventive

treatment regimens that aim to stop AD pathology before it progresses to the point at which it causes impairment.

Biology of Alzheimer's Disease

The abnormal accumulation of Aβ plaques and tau neurofibrillary tangles differentiate the AD continuum from other neurodegenerative diseases [4]. These proteins have been associated with numerous underlying neurotoxic processes that promote fibrillization, impaired cellular long-term potentiation, and synapse loss, with tau showing more direct associations and plaques potentially associated with upstream pathological processes [5,6].

Tau Protein Overview

Tau is a protein associated with microtubule stability in normally functioning neurons in the human brain. It was first isolated in 1975 and was found to colocalize with tubulin [7]. When tau becomes hyperphosphorylated, it undergoes biochemical and conformational changes that cause the proteins to form multimers and aggregate into an insoluble form known as paired helical filaments [8]. As hyperphosphorylated tau binds to tau and detaches from the microtubules, tau aggregation leads to destabilization of microtubules, thus disabling critical neuronal transport systems [9]. An advanced stage of these pathological multimers are known as neurofibrillary tangles, which are composed of paired helical filaments [10]. Post-mortem assays have shown that the quantity of neurofibrillary tangles, but not Aβ plaques, is correlated with cognitive decline and AD severity [11]. While neurofibrillary tangles have been associated with impending and ongoing neurodegeneration, neurons with marked neurofibrillary tangle pathology can survive

for years. Neuronal structural and functional capacities are negatively impacted well before cell death occurs, however [12].

It has been hypothesized that tau spreads between cells in a prion-like fashion [13]. In one such hypothesis, tau oligomers act as "seeds" that are spread trans-synaptically from the axon of a tangle-laden neuron to the distal dendrites of a hitherto unaffected neuron [14]. In AD, tau spreads throughout the brain in a stereotyped way, and regions affected throughout AD tau pathology progression are customarily categorized into Braak stages [15]. Pathological tau accumulation is first observable in the transentorhinal/entorhinal cortex (stage I), then the hippocampus (stage II), additional medial temporal regions (stage III), lateral temporal and cingulate regions (stage IV), and throughout the rest of the isocortex in frontal, parietal, and occipital regions (stages V & VI).

Amyloid-beta (Aβ) Overview

Aβ peptides constitute the other major biological hallmark of AD, insoluble senile plaques. Aβ peptides are products of membrane-bound amyloid precursor protein (APP) when APP is cleaved by the enzyme β-secretase and then γ-secretase. This cleavage yields Aβ peptides of various sizes, and peptides ending at amino acids 40 and 42 are the most prevalent products of this cleavage process [16]. Aβ1-42 peptides are especially prone to aggregating and assembling themselves into misfolded Aβ oligomers [17]. Aβ oligomers, rather than their eventual fibrillary form in senile plaques, are likely responsible for the Aβ-mediated neurotoxic effects such as increased cell membrane permeability to calcium ions and resultant cell signaling dysfunction [18,19]. As cortical AD pathology worsens and plaques increase in number, the concentration of

Aβ1-42 and other misfolded Aβ peptides decreases in the CSF, likely because of AD-related malfunctions in Aβ clearance [20].

According to histopathological studies, Aβ plaque accumulation starts in the neocortex, then spreads to the allocortex (e.g. hippocampus), and eventually to striatal regions, brain stem, and finally, in advanced AD cases, the cerebellum [21]. In cognitively normal individuals in the earliest stages of neocortical Aβ accumulation, there is not a distinct sequence in which specific brain regions or even lobes become saturated with Aβ plaques. Instead, as summarized in the literature review that I co-authored,

> "…Aβ seems to [initially] accumulate in brain regions which are highly connected [22]. Many of the earliest brain regions affected by Aβ in the disease process are members of the default mode network (DMN) and include regions such as the precuneus, medial orbitofrontal cortex, posterior cingulate cortex, anterior cingulate cortex, and angular gyrus [22–25]. The DMN comprises a network of functionally connected brain regions that are co-activated during wakeful rest and inhibited during attention-related cognitive tasks. Additionally, episodic memory retrieval is associated with increased activity of regions in the posterior DMN [26]. While the DMN has been the center of interest of most Aβ related studies, the Aβ-associated abnormal functional connectivity is not restricted to the DMN [27], and some even argue that the regions expressing early Aβ deposition are in fact regional hubs where multiple networks converge [28]. These hubs could also be the convergence point of multiple pathologies, including tau, the other pathological hallmark of AD [29,30]." [1]

Preclinical AD and CSF Phosphorylated Tau

CSF phosphorylated tau epitopes, such as those phosphorylated at threonine 181, tau phosphorylated at serine 214, and tau phosphorylated at threonine 217, are significantly elevated in patients with AD vs. controls [31]. While both CSF phosphorylated tau (CSF p-tau) and the total amount of tau in the CSF are highly correlated in AD, CSF p-tau has been reported to specifically reflect the presence of AD-related tau over other neurodegenerative diseases, while the total quantity of tau fragments in the CSF shows elevation across multiple neurodegenerative diseases [32,33]. CSF phosphorylated tau (CSF p-tau) can rise before the clinical presentation of

AD, and there is evidence that elevated levels of CSF p-tau precedes significant cortical tau accumulation in preclinical AD [34]. Currently, CSF p-tau and its associations with tau-PET tracer retention in preclinical AD is currently understudied, as the previous studies addressing this question have reported mixed results between cohorts.

Preclinical AD and Cognition

As a patient progresses through the AD continuum, a specific profile of cognitive impairment emerges. As summarized in the review that I co-authored,

> "Historically, the *in vivo* diagnosis of AD was based on the nature and the severity of cognitive impairments [35,36]. AD has been classically defined as an amnestic syndrome of the hippocampal type with a signature impairment in episodic memory retrieval that is not rectified by cueing paradigms [37]. In AD, impaired episodic memory can be manifested across a variety of cognitive faculties (free recall, recognition, paired-associate learning) and sensory modalities (auditory, visual, olfactory) [38]. AD also affects domains of language ability and semantic knowledge, including object naming, category fluency, semantic categorization, as well as working memory, attention, and visuospatial abilities [36]." [1]

By definition, individuals with preclinical AD do not present with clinically significant cognitive impairment. Nevertheless, subtle cognitive changes in preclinical AD have still been detected among cognitively normal subjects and have been associated with Aβ and/or tau pathology. A recent study showed that, within the Alzheimer's Disease Neuroimaging Initiative (ADNI) cohort, cognitively normal individuals who were positive for both CSF $A\beta_{42}$ and CSF phosphorylated tau showed worse baseline delayed verbal memory recall and executive function than Aβ+/tau- individuals, while Aβ+/tau- individuals performed worse than Aβ-/tau- individuals on these cognitive tests [39]. A meta-analysis demonstrated that cognitively normal individuals with elevated levels of Aβ deposition as measured by PET imaging, i.e. Aβ-positive individuals, showed worse performance on neuropsychological tests measuring global cognition, delayed

memory, language, visuospatial ability, and measures of working memory and executive functions compared to Aβ-negative individuals [40]. When a subset of individuals from that study were divided into more specific groups, it was shown that Aβ-positive individuals with MRI evidence of cortical neurodegeneration had worse memory performance than Aβ-positive individuals without neurodegeneration. However, the associations between AD pathology and cognitive performance among cognitively normal individuals vary in strength and even cognitive domains between studies, which could be attributable to sample differences or the use of different neuropsychological tests. This is further complicated by the lack of a distinct temporal sequence of domain-specific cognitive decline, as some individuals first show impairments in visuospatial measures, while others may first present with memory or word-finding difficulties [41,42]. There are currently ongoing efforts to develop neuropsychological measures that are more sensitive to cognitive changes in preclinical AD so that the disease can be detected as soon as possible [42,43], and it is anticipated that the development of such tests will facilitate more detailed research about cognition during this early stage of AD.

Overall, the preclinical AD is currently primarily classified by biological pathological changes that may or may not be accompanied by subclinical cognitive changes [4]. Nonetheless, subtle cognitive changes during the preclinical stage of AD occur within the same cognitive domains that are severely impaired in AD dementia, and it is noteworthy that cognitive decline is already associated with AD pathology at such an early stage of the disease.

Tau-PET Imaging with [^{18}F]Flortaucipir

While the biological side of the AD research field continues to elucidate Aβ/tau interactions, molecular conformation, pathological seeding and spreading, and kinetics of Aβ and

tau in post-mortem, animal, or *in situ* models, the imaging side of the field can use PET imaging to visualize Aβ and tau accumulation *in vivo* to examine its associations with dynamic *in vivo* factors of AD such as cognition.

> "Tau PET imaging is among the most meaningful complementary biomarkers of Aβ PET. Tau radiotracers became available for clinical research in 2012 [44], eight years after [the first commercially available Aβ radiotracer] PiB. Much like what is observed for brain atrophy and neuronal death, the topographical pattern and progression of tau deposition is distinct from that of Aβ deposition [15,45–47]. However, the presence of Aβ seems necessary for tau to spread from the medial temporal lobe to the rest of the neocortex [48–50]. The presence of both proteins is also needed for a definite diagnosis of AD dementia [4]. Thus, using Aβ PET concurrently with tau PET imaging and structural MRI may facilitate the reliable distinction of AD from other diseases in clinical settings. Current tau PET tracers also seem to reliably differentiate topographical patterns between different tauopathies [51,52]. Tau tracers are not presently approved for clinical use, however [53]." [1]

[^{18}F]AV1451, also known as flortaucipir, is a PET radiotracer frequently used in research settings to measure cortical accumulation of tau. Autoradiological and immunohistochemical studies have shown that this radioactive ligand is sensitive and binds with high avidity to hyperphosphorylated tau species, namely neurofibrillary tangle pathology. According to an immunohistochemical study, flortaucipir binding is specific to hyperphosphorylated regions of neurofibrillary tangles and appears to have variable binding strength depending on the maturity of the tangle pathology, showing higher avidity for more mature neurofibrillary tangle pathology [54]. There is mounting evidence that the tracer demonstrates nonspecific binding in brain regions such as the striatum, thalamus, and choroid plexus, and binds to non-tau compounds such as iron deposits, neuromelanin and melanin-containing cells, and brain hemorrhagic lesions [55,56]. Nonspecific binding in the choroid plexus is a particular disadvantage of this tracer as it spills over into the AD-critical hippocampus, rendering hippocampal flortaucipir binding results questionable without additional experimental corrections [57]. Nonetheless, this tracer can reliably

detect tau accumulation across the AD continuum, and its binding topography has been found to mirror post mortem tau accumulation patterns as measured by Braak stages [49,58].

When discussing PET tracer retention, it is critical to clarify how regional retention is quantified. The standardized uptake value ratio (SUVR) is a ratio of a given brain region's standardized uptake value (SUV) compared to the SUV of a region with minimal specific radiotracer uptake. An SUV is a unitless index of radiotracer uptake that reduces variability in relative tissue uptake attributable to patient's mass and the injected dosage [59]. To calculate an SUV for a prespecified ROI in the brain, one can divide the radioactivity concentration (r; kBq/ml) (i.e. the average activity per unit volume) by the quotient of the decay-corrected amount of injected radiotracer (a'; kBq) and the participant's weight (w; grams), such that SUV = r/(a'/w) [60]. SUVRs are convenient outcome measures in PET imaging because SUVR calculations do not require dynamic data, so the scanning times can be shorter and more manageable for patients and study participants [61]. In standard amyloid and tau PET imaging, SUVRs are calculated as a cortical to cerebellum SUV ratio (Knesaurek 2018). Since the cerebellum is not susceptible to tau deposition, and advanced cerebellar Aβ is rare and even then impacts the SUVR negligibly [62], segments of the cerebellum are useful reference regions in Alzheimer's PET imaging [63].

Flortaucipir in Preclinical AD: Key Studies

There is emerging evidence that flortaucipir is informative about tau pathology in the preclinical stage of Alzheimer's disease, i.e. in cognitively unimpaired individuals positive for amyloid pathology but who don't meet estimated clinical positivity thresholds for tau or show notable neurodegeneration.

In 2016, Vemuri et al. investigated intrinsic regional variability in flortaucipir signal in cognitively normal older adults [50]. They found that brain regions expressing the highest average flortaucipir SUVRs aren't necessarily the most meaningful in detecting preclinical AD-related pathology. Rather, they found that the entorhinal cortex, which shows relatively low flortaucipir SUVRs compared to other regions, was the most effective at differentiating Aβ-positive from Aβ-negative individuals.

Later in 2016, Schöll et al. determined spatial patterns of flortaucipir retention in cognitively normal individuals and its relationship to cognition and Aβ PET [49]. When examining the spatial distribution of Aβ-positive vs Aβ-negative older adults, they found that the negative individuals showed localized elevation in flortaucipir binding in the entorhinal cortex and parahippocampal gyrus, while positive individuals showed elevated flortaucipir binding in lateral temporal regions and, among some of these individuals, parietal regions. They found that Braak I/II (entorhinal and hippocampal) flortaucipir binding was sufficient to predict cross-sectional performance and longitudinal decline in episodic memory, which was replicated in a subsequent study [64]. Longitudinal decline in global cognition was predicted by higher flortaucipir binding in regions throughout the whole brain. Cross-sectional associations between flortaucipir and global cognition were not found, and neither were there any associations found with working memory nor processing speed.

In a 2017 paper, Mishra and colleagues used sparse k means clustering to determine which brain regions were most informative in detecting preclinical AD-related tau accumulation as measured by flortaucipir binding [65]. According to their sparse k means clustering analysis, the highest weighted ROIs for predicting Aβ PET positivity in cognitively normal older adults were the entorhinal cortex, lateral occipital cortex, inferior temporal cortex, and amygdala. They then

averaged the SUVRs of these regions for each participant to create a meta-ROI as a tau summary measure. This meta-ROI was correlated with episodic memory and attentional control.

There have also been conflicting results in pre-symptomatic AD research. While the following studies didn't stratify their samples by Aβ status in their analyses, some studies have found associations between regional flortaucipir binding and CSF p-tau in cognitively normal older adults, particularly in the entorhinal cortex and inferior temporal gyrus [66], while others did not find such associations in cognitively normal controls [34,67].

Biomarker Positivity and Lower Thresholds

In the AD imaging field, the term "threshold" is used in multiple contexts, particularly when defining Aβ and tau PET positivity. In several papers, "threshold" is used to describe a PET tracer SUVR that is clinically meaningful for differentiating clinical AD and MCI populations from cognitively unimpaired controls [68–70]. "Threshold" has also been used to define SUVRs that distinguish individuals with AD dementia versus individuals with non-AD neurodegenerative diseases [52]. Of most relevance to the contents of this thesis, thresholds can also refer to an SUVR that distinguishes clinically unimpaired individuals with high tracer binding vs. clinically unimpaired with low tracer binding that is pathologically, not clinically, significant [25,65]. Although there are subtle differences in the clinical implications of the aforementioned threshold definitions, they all share a common thread: distinguishing individuals with high tracer binding vs. low tracer binding. Depending on one's definition of threshold, positivity thresholds can be derived using multiple classifications methods such as AUC/ROC curves, k means clustering, and Gaussian mixture modeling [25], as well as percentiles, z-scores, and standard deviations compared to control groups [50,68].

Regardless of the Aβ-PET tracer, Aβ-PET positivity thresholds are usually quantified within a clearly defined global cortical meta-ROI [25,71]. In contrast to Aβ imaging, there is not currently a universal consensus on a robust measure or threshold for tau-PET positivity. When comparing previous studies that have explored methods for determining tau-positivity with flortaucipir, it is evident that the thresholds can vary depending on the brain region(s) used to derive the thresholds and the cohorts in which they were derived [52,65,68,69] (table i-1). However, regardless of differences in brain regions, reference regions, image processing methods, cohorts, and even different definitions of "threshold" between studies, the SUVRs of almost all of the flortaucipir thresholds reported in table i-1 fall between 1.2 and 1.4.

Tau SUVRs appear to show continuous distributions within populations, while Aβ exhibits a clearer bimodal distribution of high and low binding [68]. Therefore, it is of particular interest to investigate whether "subthreshold", or intermediate, flortaucipir binding shows meaningful associations with other proxies of AD-related pathology, even before the onset of clinical symptoms.

Brain Region(s)	**Range of reported flortaucipir threshold SUVRs**	**Reference region**	**Image processing methods**	**Paper**
Braak I/II regions	1.31 – 1.35	Inferior cerebellar gray	Non-PVC, weighted meta-ROI	Maass et al., 2017
Braak III/IV regions	1.25-1.28	Inferior cerebellar gray	Non-PVC, weighted meta-ROI	Maass et al., 2017
Braak V/VI regions	1.15-1.25	Inferior cerebellar gray	Non-PVC, weighted meta-ROI	Maass et al., 2017
Braak V/VI regions	1.21-1.28	Inferior cerebellar gray	Non-PVC, weighted meta-ROI	Ossenkoppele et al., 2018

Whole cortex	1.18-1.22	Inferior cerebellar gray	Non-PVC, weighted meta-ROI	Maass et al., 2017
Inferior temporal gyrus	1.23-1.3	Inferior cerebellar gray	Non-PVC	Maass et al., 2017
Inferior temporal gyrus	1.29-1.35	Inferior cerebellar gray	Non-PVC	Ossenkoppele et al., 2018
Entorhinal cortex	1.26-1.41	Inferior cerebellar gray	Non-PVC	Ossenkoppele et al., 2018
Temporal meta-ROI (entorhinal cortex, amygdala, fusiform, inf. temporal, & mid. temporal gyri)	1.27-1.34	Inferior cerebellar gray	Non-PVC, weighted meta-ROI	Ossenkoppele et al., 2018
Temporoparietal cortex (bilateral inferior, middle, and superior temporal gyri, banks of the superior temporal sulcus, supramarginal gyrus, transverse temporal and inferior parietal lobe)	1.21-1.27	Inferior cerebellar gray	Non-PVC, weighted meta-ROI	Ossenkoppele et al., 2018
Entorhinal cortex, amygdala, inferior temporal gyrus, lateral occipital gyrus	1.25	Whole cerebellum	PVC unweighted meta-ROI	Mishra, 2017
Entorhinal cortex, amygdala, parahippocampal gyrus, fusiform, inf. temporal, & mid. temporal gyri	1.23-1.33	Cerebellar crus gray median	Non-PVC voxel-number weighted average of the median tracer uptake in each region	Jack et al., 2017 (Alz. Dementia)

Table i-1: A summary of key studies that aimed to identify individuals with high levels of tau (i.e., positivity thresholds) as measured by regional flortaucipir retention.

While a universal tau positivity threshold has not yet been defined, flortaucipir binding in certain brain regions seem to be more related to the AD continuum than in others. A recent study showed that high flortaucipir binding in both medial and lateral temporoparietal regions most accurately distinguishes AD from other neurodegenerative diseases, and high entorhinal

flortaucipir binding best distinguishes MCI due to AD vs. MCI due to non-AD neurodegenerative diseases [52]. Therefore, it is logical to focus on such regions when considering meaningful AD-specific flortaucipir thresholds.

Family History

A family history of sporadic AD (i.e., not autosomal dominant AD) can increase an individual's risk for developing AD dementia by two- to three-fold [72,73]. When taking degree of relatedness into consideration, individuals with at least one first-degree relative (parent or sibling) affected by sporadic AD have a 1.73 relative risk of developing AD themselves compared to individuals without this family history, and individuals with four or more first-degree relatives with sporadic AD have a relative risk of 14.77 [74].

While being an apolipoprotein E (APOE) ε4 allele carrier is the strongest known genetic risk factor for late-onset AD [75,76], the increased risk due to family history may also be attributable to a combination of additional genetic and shared environmental factors [77]. Approximately 53% of phenotypic variance in late-onset AD can be explained by genetics [78], but acting on modifiable risk factors such as cardiovascular factors and low education may reduce one's risk of AD by up to 33% [79]. Therefore, cognitively intact individuals with a family history of the disease may be ideal candidates for preventive trials, especially if they have evidence of preclinical AD pathology.

Rationale for Study

So far, the literature has shown that flortaucipir binding in patients with AD dementia is associated with cortical Aβ PET binding, higher CSF p-tau, and worse cognitive performance, as

well as a myriad of other AD-specific brain signatures that are not within the scope of this study [80]. As previously summarized, recent literature further suggests that cognitively normal older adults who have high levels of cortical Aβ pathology, i.e. preclinical AD, have elevated levels of flortaucipir binding in brain regions associated with early tau accumulation. Flortaucipir's associations with CSF p-tau and cognitive performance in cognitively normal individuals have yielded mixed results between studies and cohorts. It has not been previously explored, however, if these associations are still present at lower, i.e. subthreshold, levels of flortaucipir binding, or if clinically significant levels of flortaucipir binding are necessary to observe these associations.

This study will be conducted on cognitively normal individuals from the PREVENT-AD (Presymptomatic Evaluation of Experimental and Novel Treatment of Alzheimer's Disease) cohort. The PREVENT-AD is a longitudinal study at McGill University that collects multimodal neuroimaging, biological, cognitive, and behavioral data from individuals with a familial history of sporadic AD. For this specific project, we collected flortaucipir data from 119 cognitively normal older adults at increased risk of AD due to a first-degree familial history of the disease. As a whole, this sample appears to have relatively low tau binding (median entorhinal flortaucipir SUVR = 1.05, range = 0.8-1.6). The rationale for this study is supported by the aforementioned finding that low levels of regional flortaucipir binding may not necessarily mean that no clinically meaningful information is being conveyed [50].

Hypothesis and Objectives

Our overall hypothesis is that low levels of tau could be clinically meaningful, as demonstrated by significant associations with other established measures of AD, such as Aβ PET, CSF phosphorylated tau, and cognitive performance. Moreover, we hypothesize that

associations between flortaucipir binding and the pathological biomarkers will remain present even after removing individuals with the highest levels of flortaucipir binding.

Specific aim #1: Determine if individuals positive for Aβ PET pathology have more brain region-specific flortaucipir binding than individuals negative for Aβ PET pathology.

Specific hypothesis: Aβ-positive individuals will, on average, have elevated flortaucipir binding in regions that are associated with tau pathology in sporadic AD than Aβ-negative individuals. This association will be particularly prominent in medial temporal regions.

Specific aim #2: Assess flortaucipir's relationship with phosphorylated (p)-tau in the CSF, an established biomarker of AD-related tau pathology

Specific hypothesis: Higher flortaucipir binding in similar brain regions to those associated with elevated Aβ pathology will also be associated with higher CSF p-tau levels.

Specific aim #3: Assess flortaucipir's relationship with cognitive performance, as measured by the Repeatable Battery for the Assessment of Neuropsychological Status (RBANS).

Specific hypothesis: Elevated flortaucipir binding will be associated with worse cognitive performance in multiple cognitive domains including delayed memory, but these associations won't be as strong due to the later onset of cognitive decline in the AD continuum.

Specific aim #4: Investigate the thresholds of associations between entorhinal flortaucipir binding and the previous AD measures by iteratively removing the participants with the highest entorhinal flortaucipir SUVRs.

Specific hypothesis: Aβ and CSF p-tau will begin to show associations with entorhinal flortaucipir binding at lower entorhinal flortaucipir SUVRs than cognitive performance. Therefore, the pathological biomarkers will have lower flortaucipir thresholds than the flortaucipir threshold associated with clinical expression.

CHAPTER II:

Manuscript Submitted for Publication (major revisions)

"Intermediate Flortaucipir uptake is associated with Aβ-PET & CSF-tau in asymptomatic adults"

Authors of the submitted manuscript: Melissa McSweeney*, Alexa Pichet Binette*, MSc; Pierre-François Meyer, MSc; Julie Gonneaud, PhD; Christophe Bedetti, MSc; Hazal Ozlen, BSc; Anne Labonté, BSc; Pedro Rosa-Neto, MD, PhD; John Breitner, MD; Judes Poirier, PhD; Sylvia Villeneuve, PhD for the PREVENT-AD Study Group

*=*co-first authors*

Abstract

Objective. To investigate relationships between flortaucipir [FTP] uptake, age, and established Alzheimer's disease (AD) markers in asymptomatic adults at increased risk of AD.

Methods. One-hundred-nineteen individuals with a family history of AD (PREVENT-AD cohort, mean age=67±5) underwent tau-PET ([^{18}F]FTP), Aβ-PET ([^{18}F]NAV4694 [NAV]), and cognitive assessment. Seventy-four participants also had CSF p-tau and total tau data available. We investigated the association between age and FTP in this relatively young cohort of older adults. We also investigated regional FTP SUVR differences between Aβ-positive and Aβ-negative individuals and regional correlations between FTP and NAV retention. In cortical regions showing consistent associations across analyses, we assessed whether FTP was additionally related to CSF tau and cognitive performance. Lastly, we identified the lowest FTP value at which associations with Aβ-PET, CSF and cognition were detectable.

Results. Increased age was only associated with amygdala and transverse temporal lobe FTP retention. Aβ-positive individuals had higher FTP SUVRs values in several brain regions further showing correlation with NAV load through the cortex. Increased FTP SUVRs in medial temporal regions were associated with increased CSF tau values and worse cognition. The SUVRs at which associations between entorhinal FTP SUVR and other AD markers were first detected differed by modality, with a detection point of 1.12 for CSF values, 1.2 for Aβ-PET and 1.4 for cognition.

Conclusions. Relatively low FTP-PET SUVRs are associated with pathological markers of AD in the preclinical phase of the disease. Adjustment in the tau-threshold should be considered depending on the purpose of the tau classification.

Introduction

Alzheimer's disease (AD) is characterized by the pathological accumulation of beta-amyloid (Aβ) and tau proteins starting decades before the onset of clinical impairment.[2,81,82] It is critical to understand the role of early pathology accumulation for preventive purposes. Tau-PET radiotracers, such as [^{18}F]flortaucipir (FTP), have recently permitted investigation of the topological distribution and progression of tau *in vivo*.[83,58,84,49,85,86] Little is known about the clinical validity of relatively low levels of tracer retention among cognitively normal individuals.[65]

To improve our understanding of early FTP-PET uptake and its implications in pre-symptomatic AD, we investigated associations between FTP retention and other validated AD

biomarkers in a relatively young cohort of asymptomatic older adults with at least one first-degree relative diagnosed with sporadic AD. A family history of AD increases an individual's risk by 1.7 to 14.8 fold depending of the number of first-degree relatives affected.[74] Given the slow progression of the disease and the fact that most individuals are diagnosed in their late seventy early eighty,[87] older adults within their mild sixties are the optimal target for studying early tau manifestations.

We first evaluated the association between Aβ-PET and FTP retention. We then assessed the relationships between regional FTP retention with cerebrospinal fluid (CSF) phosphorylated (p)-tau, total-tau and cognitive performance in brain regions where FTP retention was found to be associated with Aβ-PET. Finally, we evaluated whether our findings were driven by only a few individuals with high FTP SUVRs or if intermediate values are also biologically meaningful.

Methods

Participants. The present study included 119 cognitively normal late-middle aged and older adults from the Pre-Symptomatic Evaluation of Experimental or Novel Treatments for Alzheimer's Disease (PREVENT-AD) cohort.[88] PREVENT-AD is a longitudinal study of individuals who have a parent or at least two siblings diagnosed with AD-type dementia. Participants were required to 1) be at least 60 years of age, or between 55 and 59 if their age was 15 or fewer years younger than their first-affected relative's age at dementia onset, 2) have no history of major neurological or psychiatric disorders, and 3) test as cognitively normal on neuropsychological evaluation with clinical review.

Standard protocol approvals, registrations, and patient consents. This study was approved by the Institutional Review Board at McGill University. All participants provided written informed consent prior to participation.

Data availability statement. Upon request, all anonymized data and relevant documentation from this study can be made available to qualified investigators. Such an arrangement will be subject to a standard Data Sharing Agreement.

Image acquisition. FTP ([^{18}F]AV1451; Eli Lilly & Company, Indianapolis, Indiana) and [^{18}F]NAV4694 (NAV; Navidea Biopharmaceuticals, Dublin, Ohio) were used to quantify the accumulation of tau and Aβ proteins in the brain. Most PET scans were carried out on two consecutive days, and all were acquired no more than five months apart (mean delay between PET scans: 4.24 ± 16.7 days). Imaging was performed at the McConnell Brain Imaging Centre at the Montreal Neurological Institute (Montreal, Canada) between February 2017 and June 2018. Aβ scans were performed 40-70 minutes post-injection (~6 mCi), and tau scans 80-100 minutes post tracer injection (~10 mCi). T1-weighted structural MRI scans had been acquired approximately one year prior to the PET scans (mean delay: 8.9 ± 4.8 months) on a 3T Siemens Trio scanner at the Brain Imaging Centre of the Douglas Mental Health Research Institute (Montreal, Canada) using the following parameters: TR=2300ms, TE=2.98ms, number of slices=176, slice thickness=1mm.

Image processing. T1-weighted MR images were processed through FreeSurfer version 5.3[89] and parcellated according to the Desikan-Killiany atlas.[90] PET images were processed using

a standard pipeline (https://github.com/villeneuvelab/vlpp). Briefly, the 4D PET images (5min x 4 frames for FTP and 5min x 6 frames for NAV) were realigned, averaged and registered to the corresponding T1-weighted MR image. Registered PET images were then masked to exclude cerebrospinal fluid (CSF) signal and finally smoothed using a Gaussian kernel of $6mm^3$. Standardized uptake value ratios (SUVRs) used cerebellum grey matter as the reference region for Aβ scans[25,71] and the inferior cerebellum grey matter for tau scans.[57] Our analyses included the average FTP SUVRs of 34 bilateral FreeSurfer brain ROIs. The hippocampus (i.e. Braak II), thalamus, and striatum were not included in analyses due to non-specific tracer retention.[55,56] Analyses were conducted with and without correction for partial volume effect[57] and results were similar.

Amyloid positivity threshold. To quantify a global Aβ SUVR for each participant, we calculated the average SUVR from the precuneus, posterior cingulate, parietal lobe, frontal lobe, and lateral temporal regions.[25,71] A global Aβ threshold was derived using a two-component Gaussian mixture model (GMM),[25] yielding an estimated threshold of 1.37 (figure e-1). The threshold corresponds to an observation having a 90% probability of belonging to the lower Aβ distribution and a 10% probability of belonging to the higher Aβ distribution. This conservative threshold was chosen to reduce the number of false positives, but we cannot exclude the possibility that some individuals classified as Aβ-negative might in fact be Aβ accumulators and/or have meaningful subthreshold levels of Aβ. We used the *cutoff* R package (https://github.com/choisy/cutoff) to derive the estimated positivity threshold, and the *mixtools* R package (https://cran.rstudio.com/web/packages/mixtools/mixtools.pdf) to confirm the

probabilities of each observation. Twenty participants were classified as being Aβ positive (Aβ+).

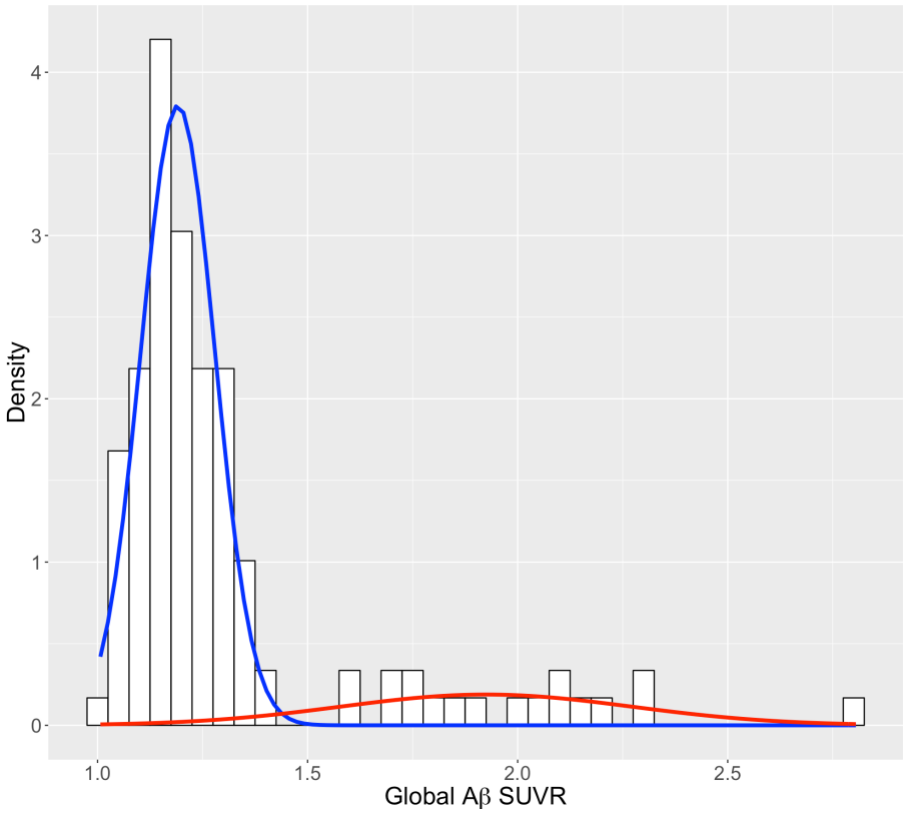

Figure e-1: Gaussian mixture modeling of global amyloid-PET distribution.
Using previously established methods, we used a two-component Gaussian mixture model to derive a cut-off SUVR for Aβ PET positivity. The cut-off value corresponds to an observation having a 90% posterior probability of belonging to the lower Aβ distribution (blue) and a 10% posterior probability of belonging to the higher Aβ distribution. Twenty out of the 119 participants (17%) exceeded the derived positivity SUVR threshold of 1.37 (90% CI 1.36-1.39) and were thus classified as Aβ-positive.

Cerebrospinal fluid analyses. A subsample of 74 individuals had undergone a lumbar puncture up to 4.5 years prior to their PET scans (mean delay=8.9 ± 9.8 months). Due to the range and variance of time differences between these two measurements, the time between lumbar puncture and PET was included as a covariate in all CSF-related analyses.

CSF p-tau (phosphorylated at threonine 181) and CSF total-tau levels were determined using a previously-described protocol.[91] In brief, lumbar punctures were performed the morning after an overnight fast, and CSF was stored in cryovial tubes at -80 degrees Celsius. CSF p-tau

and total-tau levels were assayed in duplicate using the INNOTEST ELISA (Fujirebio; Ghent, Belgium).

Neuropsychological testing. Each participant underwent a cognitive evaluation with the Repeatable Battery for the Assessment of Neuropsychological Status (RBANS)[92] within the year prior to their PET scans (3.9 ± 3.2 months). The RBANS comprises 12 subtests assigning performance to five cognitive domains: Immediate Memory (list learning and story memory), Visuospatial/Constructional Skills (figure copy and line orientation), Language (picture naming and semantic fluency), Attention (digit span and coding), and Delayed Memory (list recall, list recognition, story recall, and figure recall). Age-scaled index scores were calculated for each cognitive domain. The five index scores and the Total Scaled Index Score were used in the present study to assess the relationship between FTP retention and cognitive performance.

Statistical analyses.

We first compared demographic and clinical characteristics of the whole cohort (n=119) with the subset with CSF assays (n=74) using two-tailed Wilcoxon rank-sum tests and Chi-square tests for continuous and categorical measures, respectively. All regression models were implemented in R 3.4.1, RStudio version 1.1.383. Partial Pearson correlation coefficients were obtained using the *ppcor* R package (https://cran.r-project.org/web/packages/ppcor/index.html). The criterion for statistical significance was $\alpha \leq 0.05$ after correction for multiple comparisons. P-values from the linear models were calculated through a permutation procedure with 1000 iterations and subsequently corrected for multiple comparisons using the Benjamini-Hochberg

FDR.[93] The permutation procedure has the advantage of limiting the influence of outliers or variance differences.[94]

Age-related increase in FTP retention. Given that tau accumulation, especially in the early Braak regions, is known to increase with age (i.e. independently from AD-related process),[95] we first investigated the relationships between age and FTP SUVR in the 34 FreeSurfer brain regions (outcome variable).

Aβ and FTP associations. To determine whether Aβ+ individuals had higher FTP retention than Aβ- individuals, we analyzed the association between Aβ status (independent variable) and FTP SUVR in the 34 FreeSurfer brain regions (outcome variable) via independent linear models controlling for age and sex. To evaluate the effect size of FTP retention between Aβ+ and Aβ- participants, we calculated Cohen's *d*.

To further explore the association between Aβ and potential tau burden, we ran Pearson correlation tests between regional FTP SUVRs and regional NAV SUVRs across the 34 brain regions. We ran complete linkage hierarchical clustering to identify the regions where the associations between FTP and NAV showed similar retention patterns across regions. The regions showing consistent associations with Aβ burden in both of these analyses (higher FTP retention in Aβ+ vs Aβ- and correlating with regional NAV SUVRs) were retained as regions of interest (ROIs; FTP-ROIs) for subsequent analyses as they likely represent early AD-related tau pathology.

CSF tau and FTP associations. Next, we assessed whether FTP SUVR in the FTP-ROIs were related to CSF p-tau and CSF total-tau (independent variables) using linear regressions controlling for age, sex, and years between lumbar puncture and PET scan acquisition. Box-Cox transformation was applied to CSF p-tau and total-tau data to fulfill normality assumptions.

Cognition and flortaucipir associations. Similarly, we assessed whether FTP SUVR (independent variable) was related to age-scaled RBANS index scores (outcome variable) in the FTP-ROIs using independent linear regressions controlling for sex and education. Box-Cox transformation was applied to each of the cognitive domains to fulfill normality assumptions.

FTP SUVR detection points. As a last step, we ranked participants according to their FTP SUVRs and re-ran our linear regressions by progressively (i.e. iteratively) removing the individuals with the highest FTP SUVR, until the association between FTP SUVRs and the AD markers were lost, here referred as FTP SUVR "detection points". These analyses were performed to evaluate if associations between AD biomarkers and FTP retention were driven by high FTP SUVRs (or tau "positive" according to published thresholds[52]) or whether they reflect associations with more intermediate FTP values. We were particularly interested to know if detection points differ across the AD markers. Thus, we applied the abovementioned procedure for the linear regression between FTP SUVR and i) Aβ-PET, ii) CSF and iii) cognition. The Aβ "detection point" analysis included NAV as a continuous variable. For these specific analyses, we focused on FTP SUVR in the entorhinal cortex since it is among the earliest regions showing tau accumulation in AD.[96,97] To visualize how these detection points were associated with FTP retention in later Braak stages, we also calculated the average SUVR of the regions in Braak stages III to VI (as listed in figure 1A) and plotted these values in the same figure as the one displaying the entorhinal (Braak I) FTP SUVR detection points.

Results

Demographics. Participants' demographic and clinical characteristics are detailed in Table 1. Among the 119 participants, the mean age was 67.5 years. The subset of the participants

with both PET and CSF data were similar on all relevant measures compared to the rest of the cohort (table 1).

A)	**Whole Cohort** *(N=119)*	**CSF subsample** *(N=74)*	**statistic**	**p value**
Mean Age *y*	67.5 ± 4.8	67.2 ± 4.8	4639.5	0.53
% Female (N)	73.9% (88)	69% (51)	2.57	0.14
% *APOE4*+ (N)	40.3% (48)	41% (30)	0.03	1.00
% Aβ+ (N)	16.8% (20)	18% (13)	0.08	0.81
Mean spEYO ± SD	-5.95 ± 7.7	-6.15 ± 7.4	3847	0.62
Mean Global Aβ SUVR ± SD	1.31 ± 0.32	1.3 ± 0.26	4186	0.57
Mean EC Tau SUVR ± SD	1.08 ± 0.14	1.08 ± 0.14	4327.5	0.84
Mean Education *y* ± SD	15.1 ± 3.2	14.8 ± 2.9	4656	0.50
Mean MMSE ± SD	28.8 ± 1.2	28.8 ± 1.26	4366.5	0.92
Mean Immediate Memory Score ± SD	105.7 ± 11	106.6 ± 10.5	4130	0.47
Mean Visuospatial Score ± SD	97.4 ± 14.6	98.2 ± 13.5	4234	0.65
Mean Language Score ± SD	100.6 ± 10.4	102.9 ± 10.6	3930.5	0.21
Mean Attention Score ± SD	107.2 ± 14.2	108.4 ± 14.5	4263.5	0.71
Mean Delayed Memory Score ± SD	105.6 ± 13.5	106.1 ± 9.7	4544.5	0.71
Mean Total RBANS Score ± SD	104.4 ± 11.6	105.9 ± 11.4	4135.5	0.48
Mean CSF p-tau ± SD (µm/µl) *(N=74)*	-	55 ± 22.9	-	-

B)	**Aβ+** *(N=20)*	**Aβ-** *(N=99)*	**statistic**	**p value**	
Mean Age *y*	68.7 ± 5.7	67.2 ± 4.6	1163	0.22	
% Female (N)	65% (13)	75.8% (75)	1	0.41	
% *APOE4*+ (N)	75% (15)	34.3% (34)	11.4	**0.001**	*
% Aβ+ (N)	-	-	-	-	
Mean spEYO ± SD	-2.54 ± 7.68	-6.67 ± 7.54	1227.5	**0.04**	*
Mean Global Aβ SUVR ± SD	1.92 ± 0.35	1.19 ± 0.09	1980	**<0.001**	*
Mean EC Tau SUVR ± SD	1.21 ± 0.17	1.05 ± 0.11	1587	**<0.001**	*
Mean Education *y* ± SD	13.7 ± 2.3	15.4 ± 3.37	684	**0.03**	*
Mean MMSE ± SD	28.6 ± 1.5	28.9 ± 1.14	907	0.54	
Mean Immediate Memory Score ± SD	105.5 ± 11.4	105.8 ± 11	930	0.67	
Mean Visuospatial Score ± SD	93.5 ± 16.7	98 ± 14	819.5	0.23	
Mean Language Score ± SD	96.3 ± 8.7	101.8 ± 10.9	762.5	0.1	
Mean Attention Score ± SD	104.9 ± 15.3	107.7 ± 14	849	0.32	
Mean Delayed Memory Score ± SD	102.2 ± 13.2	107.5 ± 9	814	0.21	
Mean Total RBANS Score ± SD	100.1 ± 11.9	105.5 ± 11.5	742	0.08	
Mean CSF p-tau ± SD (µm/µl) *(N=74)*	80.6 ± 27.9	49.5 ± 17.7	686	**<0.001**	*

Table 1: Demographics Summary.
Demographic and clinical characteristics of the cohort, comparing **A)** the whole cohort vs. the subsample of individuals with recent CSF data and **B)** Aβ-positive vs. Aβ-negative participants. Wilcoxon rank-sum tests were

performed on continuous measures (statistic = Wilcoxon's W), and Chi-square (statistic = χ^2) on categorical measures. Significant values are indicated in bold text. MMSE=Mini Mental State Exam, EC= entorhinal cortex, spEYO= years to estimated symptom onset (sporadic AD) (participant's age – age of relative at symptom onset).

Association between age and FTP retention. Older age was only associated with increased amygdala (r=0.33, p=0.002) and transverse temporal lobe (r=-0.30, p=0.001) FTP retention.

Association between NAV and FTP retention. Higher FTP retention in Aβ+ individuals was observed in 14 cortical regions (figure 1A; table 2). A Cohen's *d* value > 0.8 suggested a large effect of Aβ status on FTP retention in medial temporal regions, *viz.*, entorhinal cortex, amygdala, and parahippocampal gyrus, thus encompassing Braak stage I/III regions (table 2). The hippocampus, which constitutes Braak stage II, was excluded from these analyses due to the aforementioned non-specific binding. Aβ status showed an apparent medium effect ($0.5 \leq$ Cohen's $d \leq 0.8$) on FTP retention in the fusiform gyrus, lingual gyrus, inferior temporal gyrus, middle temporal gyrus, isthmus cingulate, lateral occipital gyrus, inferior parietal lobe, superior temporal gyrus, banks of the superior temporal sulcus, and pericalcarine cortex (Braak stage III to VI regions, table 2). A small effect of Aβ status was observed in the precuneus. The correlation matrix in Figure 1B shows that eight of these 14 brain regions further showed robust associations with NAV retention throughout the cortex and were clustered together. The remaining regions, while still showing some associations with NAV retention in many regions, were part of different clusters with weaker correlations. Given that AD-related tau propagation is hypothesized to be Aβ-dependent, the subsequent analyses are restricted to FTP retention in the top cluster, which includes eight ROIs: the entorhinal cortex, amygdala, the parahippocampal and fusiform gyri, the inferior and middle temporal gyri, lateral occipital gyrus, and inferior parietal lobe (FTP-ROIs, figure 1C).

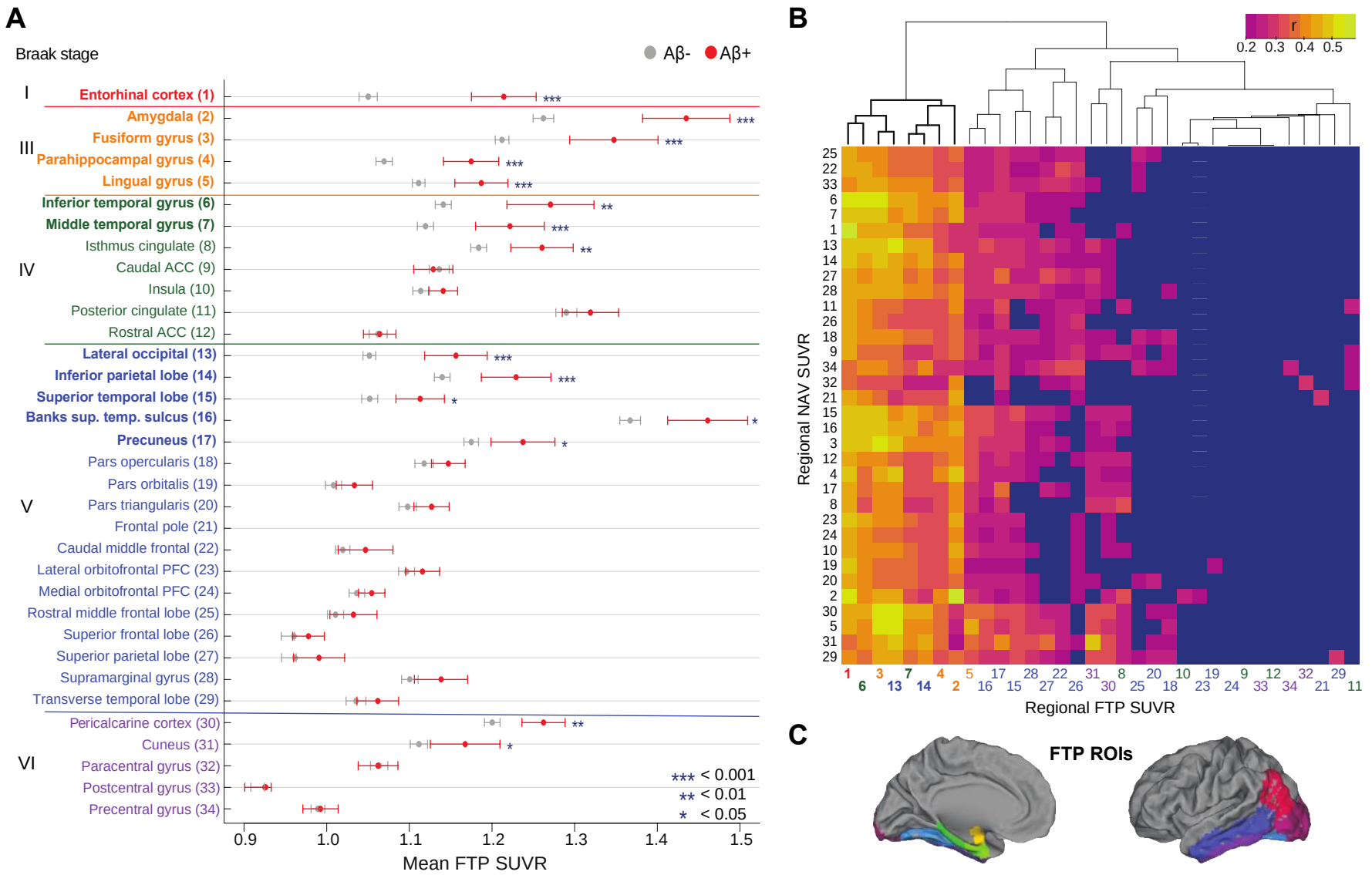

Figure 1: Higher flortaucipir uptake in several medial and lateral posterior cortical regions are associated with Aβ retention.
1A) Mean flortaucipir SUVRs across the FreeSurfer Desikan regions, organized and color-coded by Braak stages, in global Aβ+ (red) and global Aβ- (gray) groups and their respective standard error bars. Asterisks indicate the regions in which the flortaucipir SUVR is higher between the Aβ+ and Aβ- groups (post-FDR correction).

1B) Heat plot of the regional Pearson correlation coefficients between regional flortaucipir retention and regional NAV retention. The cells in dark blue represent regions with correlation test p-values that did not survive FDR-correction. We applied complete linkage hierarchical clustering to correlation coefficients surviving FDR correction to identify

regions with similar FTP-NAV uptake correlation patterns. Regions are labeled with numbers corresponding to the numbers in figure 1A, and the flortaucipir regions are color-coded by Braak stage corresponding to figure 1A. The dendrogram branches of the most consistent flortaucipir-Aβ associations clustered together and are emphasized in bold.

1C) Projected onto a brain template are the eight "FTP-ROIs" that showed a reliable pattern between the group analyses presented in 1A and the cluster analysis presented in 1B. These eight regions showed increased FTP uptake in the analyses comparing Aβ+ to Aβ-, and they are also the brain regions showing the highest and most consistent regional associations between NAV and FTP and are the focus of the subsequent analyses.

	ROI	p-value	Cohen's D	t-score
Braak I	**Entorhinal Cortex**	**<0.001**	1.121	5.311
Braak III	**Amygdala**	**<0.001**	0.916	4.524
	Fusiform gyrus	**<0.001**	0.757	4.617
	Parahippocampal gyrus	**<0.001**	0.834	4.101
	Lingual gyrus	**<0.001**	0.663	3.885
Braak IV	**Inferior temporal gyrus**	**0.001**	0.722	4.113
	Middle temporal gyrus	**<0.001**	0.688	3.587
	Isthmus cingulate	**0.004**	0.559	2.891
	Caudal anterior cingulate gyrus	0.973	-0.064	-0.039
	Insula	0.264	0.313	1.158
	Rostral anterior cingulate gyrus	0.883	0.020	0.135
Braak V	**Lateral occipital gyrus**	**<0.001**	0.798	4.662
	Inferior parietal lobe	**<0.001**	0.601	3.386
	Superior temporal lobe	**0.011**	0.533	2.649
	Banks of the superior temporal sulcus	**0.004**	0.531	2.830
	Precuneus	**0.017**	0.457	2.560
	Frontal pole	0.271	0.246	1.116
	Caudal middle frontal gyrus	0.261	0.227	1.153
	Lateral orbitofrontal PFC	0.432	0.205	0.817
	Medial orbitofrontal PFC	0.438	0.215	0.813
	Rostral middle frontal lobe	0.306	0.191	1.070
	Superior frontal lobe	0.243	0.301	1.205
	Superior parietal lobe	0.098	0.316	1.747
	Supramarginal gyrus	0.122	0.305	1.671
	Posterior cingulate	0.341	0.208	0.936
	Transverse temporal lobe	0.137	0.227	1.499
	Parsopercularis	0.223	0.290	1.222
	Parsorbitalis	0.344	0.260	0.960
	Parstriangularis	0.243	0.288	1.197
Braak VI	**Pericalcarine cortex**	**0.008**	0.586	3.071
	Cuneus	0.03	0.368	2.355
	Paracentral gyrus	0.958	-0.013	-0.045
	Postcentral gyrus	0.766	0.003	0.303
	Precentral gyrus	0.757	0.035	0.273

Table 2: Table of statistics for flortaucipir uptake in Aβ-positive (+) vs Aβ-negative (-) individuals.
Corresponds to Figure 1. Desikan FreeSurfer regions are organized by their respective Braak stage. The p-values of regions with significantly elevated tau in Aβ+ vs Aβ- individuals that survive FDR correction are indicated in bold text. The reported t-scores are the raw scores from the non-permuted regressions and the reported p-values are from permutations before FDR correction. Significant p-values and corresponding regions that survived FDR correction are indicated in bold tex

Association between CSF tau values and FTP retention. CSF p-tau was associated with higher FTP retention in six out of the eight FTP-ROIs (Table 3). Again, the strongest association was observed in the entorhinal cortex. CSF p-tau was also associated with FTP retention in the amygdala, fusiform, parahippocampal gyrus, inferior temporal gyrus, and lateral occipital gyrus (figure 2A, 2C; table 3). The regional associations between FTP retention and CSF total-tau were identical, which could be due to the strong correlation between CSF p-tau and total-tau levels in this cohort (Spearman r=0.95).

	ROI	p-value	partial correlation	t-score
Braak I	**Entorhinal Cortex**	**<0.001**	0.524	5.110
Braak III	**Amygdala**	**0.006**	0.352	3.124
	Fusiform Gyrus	**<0.001**	0.414	3.779
	Parahippocampal Gyrus	**0.007**	0.322	2.828
Braak IV	**Inferior Temporal Gyrus**	**0.016**	0.311	2.714
	Middle Temporal Gyrus	0.167	0.168	1.416
Braak V	**Lateral Occipital Gyrus**	**0.016**	0.280	2.418
	Inferior Parietal Lobe	0.881	0.019	0.160

Table 3: Table of correlations for flortaucipir and CSF p-tau levels.
Summary of linear regressions evaluating associations between regional FTP uptake and CSF p-tau. Corresponds to Figure 2A, 2C. Only the eight FTP-ROIs were included in the current analyses. Linear regressions and partial correlation coefficients were controlled for age, sex and years between lumbar puncture and FTP scan. Significant p-values surviving FDR correction are indicated in bold text.

Association between cognitive performance and FTP retention. The delayed memory index showed the strongest associations with FTP retention. Lower memory scores were associated with higher FTP retention predominantly in the Braak I/III regions (figure 2B, 2D; table 4). Higher FTP SUVRs in subsets of the FTP-ROIs were also associated with language, visuospatial/constructional, and total RBANS index scores (figure e-2; table e-4), but there were no associations with immediate memory or attention index scores. The entorhinal cortex was the

only region associated with all four of the cognitive index scores that showed association with FTP retention.

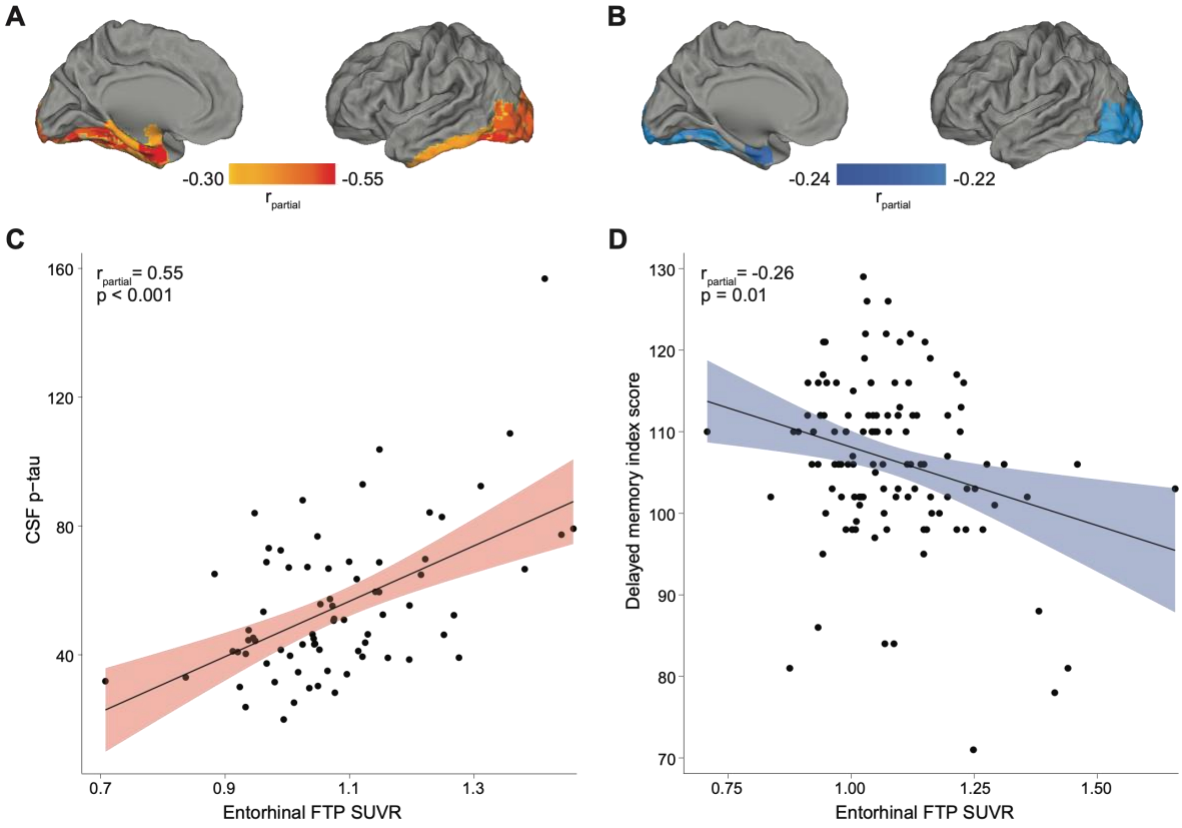

Figure 2: flortaucipir uptake in several brain regions are associated with greater levels of CSF p-tau and worse delayed memory.
2A) Partial correlation coefficients of the regions associated with CSF p-tau (Box-Cox transformed) projected onto a brain template. Only the eight ROIs presented in Figure 1C were included in the current analysis. Partial Pearson correlations were performed on a regional basis and adjusted for age, sex and years between lumbar puncture and FTP scan.
2B) Partial correlation coefficients of the regions associated with lower age-scaled delayed memory performance (Box-Cox transformed) on the Repeatable Battery for the Assessment of Neuropsychological Status (RBANS) projected onto a brain template. Only the eight ROIs presented in Figure 1C were included in the current analyses. Partial Pearson correlations were performed on a regional basis and adjusted for sex and education.
2C) Higher entorhinal FTP SUVR is associated with higher CSF p-tau. Entorhinal FTP uptake had the strongest association with CSF p-tau among the eight ROIs in this analysis. The 95% confidence interval is indicated in red and the non-transformed CSF p-tau values are presented. N participants with CSF data = 74.
2D) Higher entorhinal FTP SUVR is associated with a lower delayed memory index score. Entorhinal FTP uptake had the strongest association with delayed memory among the eight ROIs in this analysis. The 95% confidence interval is indicated in blue and the non-transformed delayed memory scores are presented. N participants with neuropsychological data = 119.

	ROI	p-value	partial corr.	t-score
Braak I	**Entorhinal Cortex**	**0.009**	-0.245	-2.714
Braak III	Amygdala	0.037	-0.195	-2.135
	Fusiform Gyrus	**0.013**	-0.224	-2.468
	Parahippocampal Gyrus	0.09	-0.156	-1.699
Braak IV	Inferior Temporal Gyrus	0.137	-0.139	-1.508
	Middle Temporal Gyrus	0.272	-0.106	-1.145
Braak V	**Lateral Occipital Gyrus**	**0.012**	-0.222	-2.447
	Inferior Parietal Lobe	0.122	-0.142	-1.541

Table 4: Table of correlations for flortaucipir and delayed memory performance.
Summary of linear regressions evaluating associations between regional FTP uptake and the age-scaled RBANS delayed memory index score. Corresponds to Figure 2B, 2D. Only the eight FTP-ROIs were included in the current analyses. Linear regressions and partial correlation coefficients were controlled for sex and years of education. Significant p-values and corresponding regions that survived FDR correction are indicated in bold text.

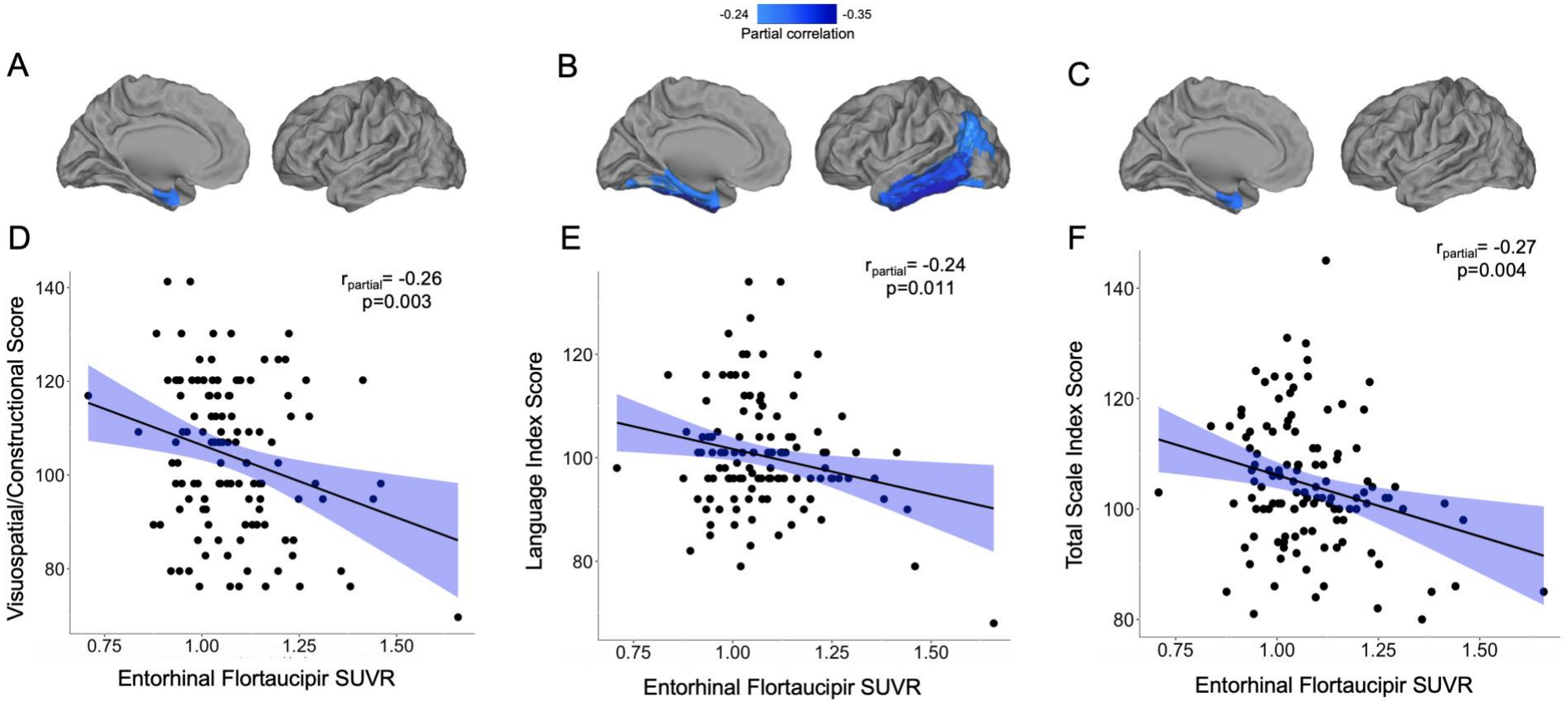

Figure e-2: Flortaucipir binding is associated with lower domain-specific cognitive performance.
A-C: Partial correlation coefficients projected onto a brain template, adjusted for sex and education, of the regions with higher flortaucipir binding associated with lower age-scaled A) visuospatial/constructional scores, B) language index scores, and C) total RBANS scores. Partial correlation coefficients for each cognitive domain were calculated from Box-Cox transformed cognitive scores. Only associations that survived FDR correction for multiple comparisons are projected onto the brains. *RBANS=Repeatable Battery for the Assessment of Neuropsychological Status.*
D-F: Scatterplots of the associations between entorhinal flortaucipir SUVR and D) visuospatial/constructional scores, E) language index scores, and F) total RBANS scores. The statistics were derived with Box-Cox transformed cognitive scores, but the untransformed scores are presented on the y-axis to facilitate clinical interpretation.

		Visuospatial/Constructional			Language			Total Score		
	ROI	**p-value**	**partial corr.**	**t-score**	**p-value**	**partial corr.**	**t-score**	**p-value**	**partial corr.**	**t-score**
Braak I	Entorhinal Cortex	**0.003**	-0.259	-2.874	**0.011**	-0.239	-2.634	**0.004**	-0.269	-2.991

Braak III	Amygdala	0.188	-0.125	-1.350	0.071	-0.162	-1.760	0.13	-0.146	-1.585
	Fusiform Gyrus	0.035	-0.199	-2.180	**0.008**	-0.269	-2.990	0.026	-0.204	-2.238
	Parahippocampal Gyrus	0.07	-0.166	-1.804	**0.01**	-0.244	-2.696	0.084	-0.171	-1.856
Braak IV	Inferior Temporal Gyrus	0.038	-0.194	-2.122	**0.001**	-0.346	-3.950	0.013	-0.227	-2.504
	Middle Temporal Gyrus	0.048	-0.190	-2.080	**0.003**	-0.321	-3.639	0.04	-0.183	-2.000
Braak V	Lateral Occipital Gyrus	0.312	-0.087	-0.934	0.103	-0.156	-1.689	0.087	-0.159	-1.731
	Inferior Parietal Lobe	0.279	-0.101	-1.086	**0.011**	-0.248	-2.744	0.057	-0.179	-1.955

		Immediate Memory			**Attention**		
	ROI	**p-value**	**partial corr.**	**t-score**	**p-value**	**partial corr.**	**t-score**
Braak I	Entorhinal Cortex	0.242	-0.114	-1.227	0.803	-0.023	-0.249
Braak III	Amygdala	0.291	-0.098	-1.053	0.409	0.080	0.861
	Fusiform Gyrus	0.322	-0.092	-0.995	0.423	0.077	0.830
	Parahippocampal Gyrus	0.39	-0.081	-0.875	0.561	0.057	0.615
Braak IV	Inferior Temporal Gyrus	0.349	-0.082	-0.887	0.814	-0.022	-0.231
	Middle Temporal Gyrus	0.448	-0.071	-0.760	0.706	0.036	0.387
Braak V	Lateral Occipital Gyrus	0.156	-0.128	-1.386	0.601	0.049	0.530
	Inferior Parietal Lobe	0.316	-0.094	-1.017	0.623	-0.044	-0.471

Table e-4: Table of statistics for flortaucipir binding and domain-specific cognitive performance. Corresponds to Figure e-2. Values are based on Box-Cox-transformed cognitive data. There were significant associations between flortaucipir binding in FTP regions and language, visuospatial/constructional, and total RBANS index scores, but not with immediate memory or attention index scores. The p-values of associations that survived FDR-correction for multiple comparisons are indicated in bold text

Detection points for FTP SUVR associations vary across modalities. To investigate to which extent the associations found between FTP retention and Aβ burden, CSF tau and cognition were influenced by high FTP SUVRs, we assessed the entorhinal FTP SUVRs at which these associations were lost. The highest entorhinal FTP SUVR detection point was for cognition, with the associations with the delayed memory index score being lost at an SUVR of 1.41 (figure 3A). Detection points for the other cognitive domain scores were in the same range (1.36, 1.66, and 1.38 for visuospatial/constructional, language, and total RBANS scores respectively). The FTP SUVR detection point for associations with global NAV SUVR was at 1.23, and the detection point for associations with both CSF p-tau and CSF total tau was as low as 1.12. Interestingly, the four individuals exceeding the delayed memory detection point (entorhinal FTP SUVR $\geq$ 1.41) also had the highest mean SUVRs in later Braak stages (figure 3B).

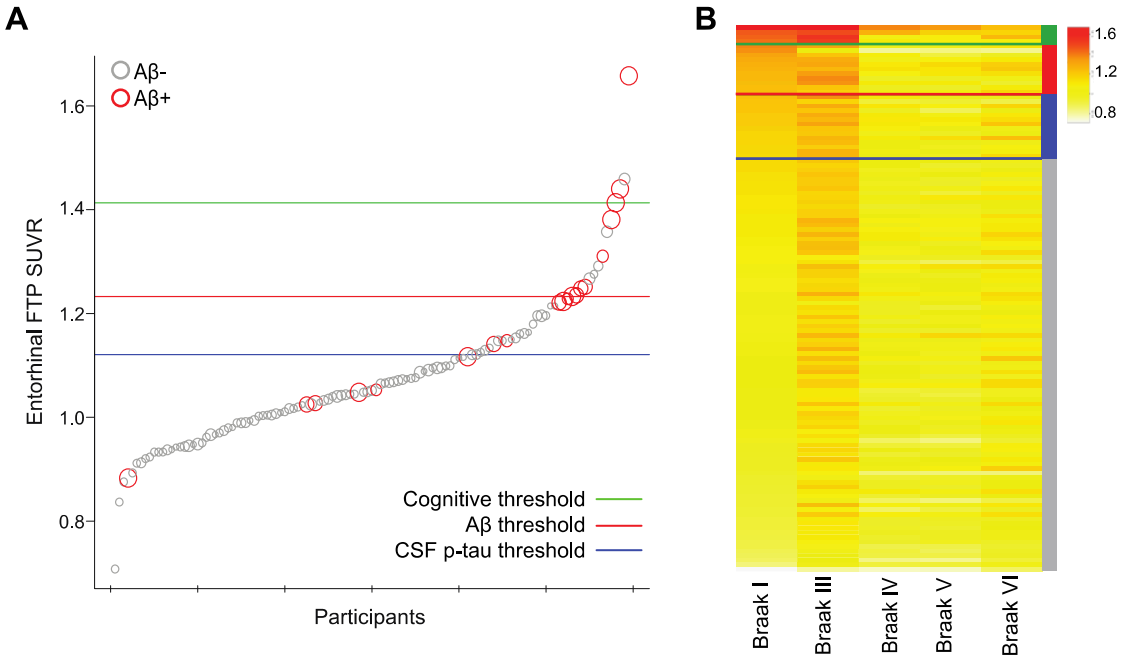

Figure 3: Relatively low entorhinal flortaucipir SUVR values are associated with CSF p-tau and Aβ-PET uptake while worse cognition is driven by individuals with higher entorhinal flortaucipir uptake.

3A) Individual participants are ranked in order of entorhinal FTP uptake. Global Aβ-positive individuals are indicated in red, and Aβ-negative individuals are in gray. The size of the data points is reflective of each individual's Aβ-PET SUVR, with larger sizes indicating higher SUVRs. The horizontal lines indicate at which entorhinal FTP SUVR values the associations between CSF p-tau (blue), continuous Aβ-PET (red), and delayed memory (green) are first detected. These detection points were obtained by iteratively running linear regressions (with 1000 iterations of permutations) and removing the participant with the highest entorhinal FTP SUVR for each iteration.

3B) Individual participants are ranked in order of entorhinal FTP (Braak I) uptake in descending order. For each participant, we calculated the mean SUVRs of the regions in Braak stages III-VI to visualize global tau distribution in individuals who fell above the delayed memory, Aβ, and/or CSF p-tau detection points. The delayed memory detection point was only reached in individuals who had high tau uptake (>1.4) in Braak stages equal to or higher than stage III.

Discussion

Cross-sectional studies have estimated that changes in CSF tau can be detected about 15 years before disease onset in autosomal dominant AD.[98] In the last decade, different classes of

tau-PET tracers have been developed, the most widely used one being FTP. The goal of this study was to assess early associations of FTP retention with other well-established pathological and clinical AD biomarkers in a cohort of relatively young (mean age 67.5 years old), cognitively healthy older adults at increased risk for AD dementia. Considering that about half of sporadic AD dementia patients are diagnosed between 75 and 84 years old,[87] older adults within their sixties are an ideal population in which to study early tau accumulation.

With the objective of identifying individuals with evidence of tau pathology using PET imaging, several studies have aimed to define a threshold for tau positivity. Even though FTP positivity thresholds are not fully comparable between cohorts due to methodological differences (e.g., data collection, region(s) of interest, images preprocessing, analyses), most reported medial temporal thresholds fall between 1.25 and 1.4.[52,65,68,69] Based on these published thresholds, the PREVENT-AD cohort shows relatively low FTP retention, with only 9% of the participants showing entorhinal SUVRs above 1.25 (median entorhinal SUVR 1.05, range 0.71-1.67), leaving the vast majority of the participants with what could be qualified as "subthreshold" values. We show that these apparently small elevations in FTP retention are already related to an ongoing pathological process, as reflected by the robust associations with Aβ-PET, CSF p-tau and total-tau. More importantly, our detection points for Aβ and CSF (both p- and total-) tau were as low as 1.23 and 1.12, respectively. As it is more and more acknowledged in the field of Aβ-PET, [99,100] subthreshold or intermediate FTP values shouldn't be discarded in the context of research or clinical trials because, in some individuals, they might reflect early pathological processes, a finding that will need to be validated by autopsy studies.

Autoradiographic and immunohistochemical studies have suggested that FTP binds with high avidity to tau paired helical filaments and neurofibrillary tangles in AD brains, while

showing minimal binding to Aβ or deposits of straight tau filaments in non-AD tauopathies.[54,101] FTP tracer retention patterns have been found to mirror Braak tau staging in older individuals across the AD spectrum[49,85,86,102] and are correlated with clinical and neuroanatomical variability in distinct AD variants.[103] We found increased FTP uptake in Braak stages I/III in addition to a subset of Braak stages IV to VI in Aβ+ individuals as compared with Aβ- individuals. In general, the strengths of these associations followed the known progression and distribution of aggregated tau in the brain.[96] Of importance, these associations were present when controlling for age, suggesting that our findings are more likely to reflect an AD-related process than (only) age-related tauopathy. The association between FTP retention and age was in fact relatively sparse and restricted to amygdala and transverse temporal lobe uptake. This finding is in line with previous results also reporting a strong association between increased age and elevated FTP binding in amygdala.[49,86]

To further explore the regional pattern of associations between NAV and FTP tracer retention, we computed a correlation matrix and used hierarchical clustering to identify brain regions in which FTP uptake was associated with NAV uptake. Assuming that Aβ leads to the cortical spreading of tau ,[3] only brain regions expressing such associations should capture AD-related tau. Increased FTP tracer uptake in eight brain regions that showed elevated FTP tracer retention in Aβ+ individuals were also associated with increased NAV retention throughout the cortex. These eight regions (entorhinal cortex, amygdala, parahippocampal and fusiform gyri, inferior and middle temporal gyri, lateral occipital gyrus, and inferior parietal lobe) are known to exhibit post-mortem tau neurofibrillary tangle distribution in sporadic AD in Braak stages I-V.[96,97]

We found that higher CSF p-tau was associated with increased FTP retention in medial temporal, lateral temporal, and occipital regions. Elevated CSF p-tau has high sensitivity and specificity for AD dementia, as it distinguishes AD from other tauopathies and is elevated in patients when compared to normal controls.[104] In our experiment, a subset of structures affected by tau in Braak stages I and III had the strongest associations with CSF p-tau levels. The associations with total-tau were extremely similar, which can be explained by the almost perfect correlation between both tau CSF markers reported here and by others.[31,105]

Previous work assessing the relationships between FTP retention and CSF p-tau in cognitively normal older adults have found varying strengths of associations,[34,66,67] including several groups reporting an absence of associations between FTP retention and CSF p-tau among cognitively normal controls.[67,34] Such discrepancies may be attributable in part to the younger age of the cohort and differences in risk factors between cohorts. Overall, the PREVENT-AD cohort is composed of individuals with a family history of sporadic AD, and thus individuals in this sample are more likely to be on a path toward AD than a sample randomly selected from the general population. Participants are also about 10 years younger than most other cohorts investigating tau-PET in preclinical late onset AD,[34,50,106] including the well-known Alzheimer's Disease Neuroimaging Initiative study (http://adni.loni.usc.edu; mean age of cognitively normal participants with flortaucipir data = 75.42 ± 7.53).

Finally, higher FTP SUVRs were associated with lower delayed memory, language, visuospatial/constructional, and total RBANS scores. These associations were all driven by only a few cases with the highest FTP SUVRs in the entorhinal cortex. Of interest, these cases also had among the highest SUVRs in advanced Braak stages. This finding aligns with previous work showing that global cognitive decline is associated with the spread of tau in isocortical regions

beyond the limbic network and medial temporal lobe.[49] More specifically, it suggests that small increases in entorhinal FTP retention reflect an ongoing pathological process that is still in an early phase, while higher levels of tau along with propagation to later Braak stages are needed to affect cognitive functioning. The fact that the detection points for cognitive associations were higher than the detection points for CSF tau and Aβ associations raises the question if FTP thresholds to define positivity should vary depending on the purpose of the study. For example, while higher thresholds might be optimal to detect individuals close to or already entering the clinical phase of the disease, lower thresholds might be favored in clinical trials to target the best candidates to anti-tau therapies.

In summary, FTP retention in Braak stages I, III, and the lateral occipital gyrus were consistently associated with the established AD biomarkers we studied, as well as cognitive performance. The predominant place of the Braak V lateral occipital gyrus in our analyses, although previously reported by others,[65] warrants further investigation. A key and novel finding in this study is that the associations of FTP retention with Aβ-PET and CSF p-tau emerge when individuals have relatively low entorhinal FTP SUVRs. These findings may point toward an intermediate stage of FTP retention in which early tau elevation, going as low as 1.23 if we assume that Aβ is needed for tau propagation in AD, indicates early AD-related pathological changes. These intermediate cases would not yet express the clinical manifestation of the disease, but they would nevertheless be a critical target population for anti-tau clinical trials.

Chapter III

Discussion: Future Directions and the Broader Implications of Identifying Preclinical AD with PET Imaging

Contributions to the Literature

In summary, the contents of this thesis confirm previous findings that cognitively normal Aβ+ individuals have higher flortaucipir retention than Aβ - individuals, especially in medial temporal regions such as the entorhinal cortex. Additionally, it adds to the evidence supporting the existence of preclinical associations of flortaucipir with cognitive performance and CSF p-tau. Of most novelty, it demonstrates that entorhinal flortaucipir binding has differing thresholds at which it becomes pathologically relevant to well-established AD markers. While the association between higher entorhinal flortaucipir and worse delayed memory were primarily driven by individuals who surpassed previously established AD-related thresholds, the entorhinal flortaucipir thresholds for Aβ and CSF p-tau in this study took on lower values. Together, this suggests that intermediate levels of flortaucipir retention can detect burgeoning pathological associations preceding clinical trends of cognitive decline early on in the AD continuum, a finding that will need to be confirmed with post-mortem assays of neurofibrillary tangle burden. This supports the argument that cognitively normal individuals with intermediate levels of flortaucipir uptake should be included in anti-tau clinical trials.

Future Directions

The findings presented in this manuscript raise additional questions that should be addressed in future studies in order to further understand the implications of intermediate flortaucipir retention. Several points that should be addressed include 1) measures of

neurodegeneration and regional flortaucipir in preclinical AD, 2) longitudinal cognition, 3) evaluating the relationship between Aβ and regional flortaucipir retention at a lower Aβ-positivity threshold, 4) considering the underexplored association of CSF p-tau and cortical Aβ, and 5) evaluate flortaucipir retention in advanced Braak stages.

Neurodegeneration and flortaucipir retention. A next logical step would be to examine the associations between regional flortaucipir retention and measures of neurodegeneration, such as cortical thickness. According to the expected sequence of biological changes in AD, cortical neurodegeneration should follow the pathological accumulation of Aβ and tau pathology [4]. Moreover, neurodegeneration has been tightly associated with the presence of tau pathology in multiple neurodegenerative diseases including AD [107], and hyperphosphorylated tau species have been linked to downstream biochemical processes that mediate cell death [108].

To address this highly relevant topic, we ran an exploratory partial correlation analysis (adjusted for age and sex) to visualize associations between regional flortaucipir retention and regional cortical thickness (figure 4A). Given the predominant position of entorhinal flortaucipir retention in our analyses, we further visualized the association between this measure and entorhinal cortical thickness (figure 4B). None of the associations between regional cortical thickness and flortaucipir retention survived FDR correction. There was a weak negative association between entorhinal flortaucipir retention and cortical thickness (r partial=-0.22), but the association was not statistically significant (p=0.061).

Although these cross-sectional analyses did not reveal substantial evidence for associations between flortaucipir retention and neurodegeneration in this cohort, this question should be explored further with longitudinal cortical thickness data in future studies. This is

because some individuals may start out with varying cortical thickness measurements due to latent factors such as brain reserve [109], and thus individual slopes of cortical thickness changes would provide more meaningful information.

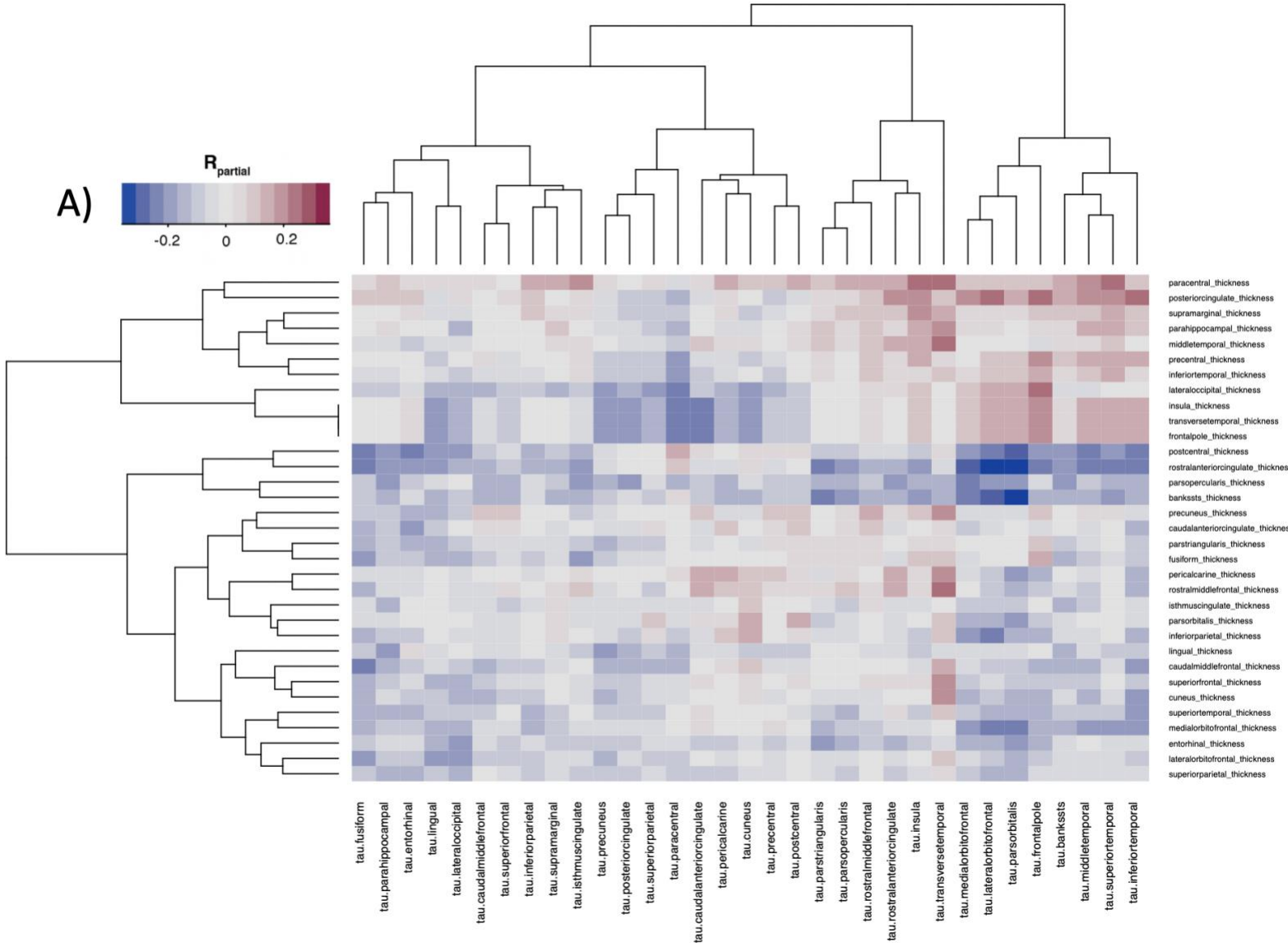

Figure 4A: Cortical thickness and FTP partial correlation matrix. Partial correlation coefficients between regional FTP retention (x-axis) and cortical thickness (y-axis), adjusted for age and sex, are projected onto a correlation matrix with complete linkage hierarchical clustering.

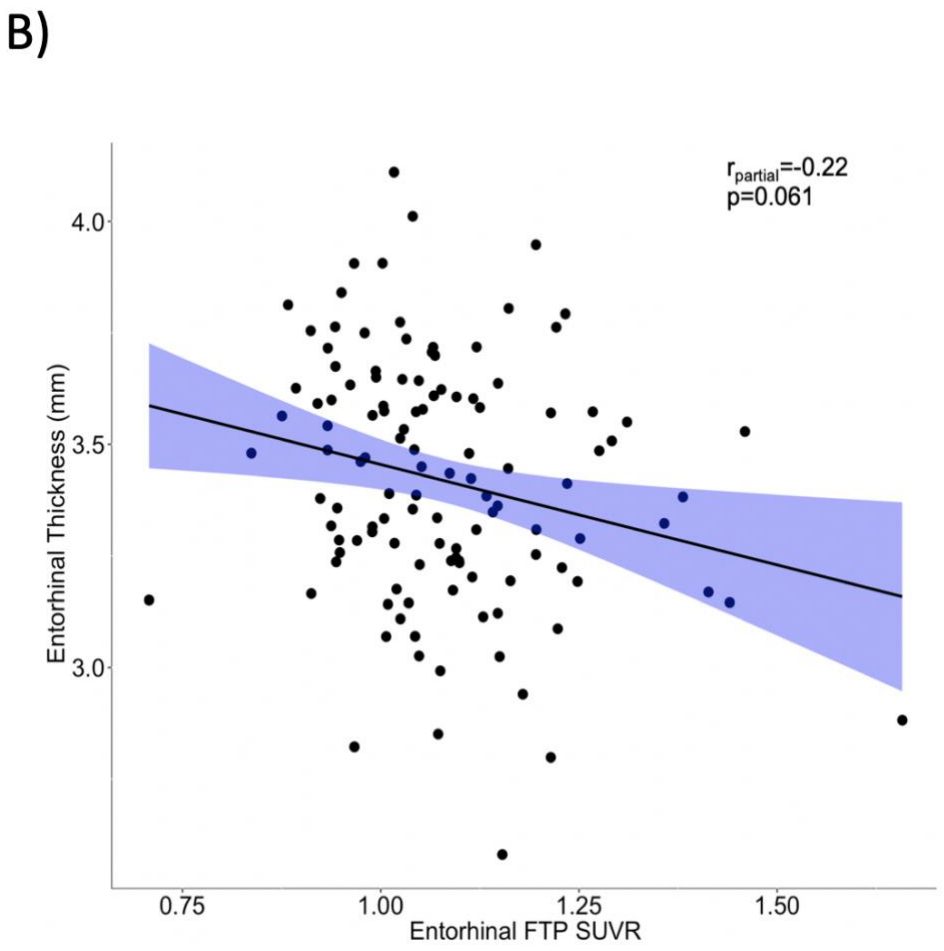

Figure 4B: Association between entorhinal FTP retention and entorhinal cortical thickness. A scatterplot is plotted between entorhinal FTP retention and its corresponding cortical thickness.

Longitudinal cognitive decline. In this study, the four individuals with the highest level of entorhinal flortaucipir binding (SUVR $\geq$ 1.41) appeared to have driven the association with delayed memory. It would be interesting to explore in future studies if these individuals in this cohort also have the most severe longitudinal cognitive decline, as it has recently been shown that longitudinal cognitive decline is associated with flortaucipir retention in preclinical AD [110]. Moreover, recent studies have shown that Aβ+ individuals with higher flortaucipir binding have more severe longitudinal cognitive decline than Aβ – individuals [110,111].

In a more novel direction, as post-PET scan cognitive data are continuing to be collected from the PREVENT-AD cohort, it would be interesting to conduct a prospective study to see if individuals who exceeded a certain entorhinal flortaucipir SUVR would be more likely to experience future cognitive decline. This would present an even stronger argument that individuals presenting as cognitively normal with fairly low flortaucipir retention would be highly valuable to include in anti-tau clinical trials.

Lowering the Aβ-positivity threshold. Despite this sample's elevated risk of AD given their first-degree familial history of the disease, only 17% of them were classified as Aβ-positive. We hypothesize that this fairly low proportion may be attributable to the conservative Aβ-positivity threshold we utilized. Too be consistent with previous studies examining the associations between flortaucipir binding and Aβ+ PET, we quantified Aβ-positivity with a global measurement of Aβ. In this specific experiment we wanted to look at individuals with clinically significant levels of global Aβ pathology in order to assess the relationship between flortaucipir binding in cognitively normal individuals with low flortaucipir binding. Since we wanted to make sense of binding that is already low, we chose a clear measure of Aβ pathology to avoid biasing our results with potential spurious associations.

In support of this conservative threshold, the global Aβ SUVRs take on a bimodal distribution (figure e-1) in which Aβ+ individuals clearly fall into a distinct distribution from the rest of the sample, which was substantiated by the threshold derived in the Gaussian mixture model. The 1.37 positivity threshold we derived in this experiment is similar to a previously estimated positivity threshold calculated for the NAV Aβ PET tracer that differentiated individuals with mild cognitive impairment from cognitively normal controls [70]. Nonetheless, it

would be worthwhile to explore the associations between intermediate global Aβ and regional flortaucipir-binding in future studies.

Although this question is outside of the immediate scope of this study, we ran a subsequent preliminary evaluation of other methods of classifying Aβ positivity, such as checking two standard deviations above the mean global Aβ index of 11 younger adults for a global Aβ-positivity threshold value of 1.225. In this case, 65 participants exceeded this threshold, and all of the 34 tested Desikan-Killiany atlas regions except the frontal pole had elevated flortaucipir binding in Aβ+ compared to Aβ - individuals. We also ran the analyses with a threshold based on the precuneus NAV SUVR alone for a threshold of 1.489, as this region has consistently been shown to be among the earliest to exhibit Aβ plaque pathology [25,112]. This threshold was derived using the same Gaussian mixture model method and parameters as we used to estimate the global Aβ threshold in the manuscript. Thirty-seven participants exceeded this value. Here, we observed significant associations between regional FTP binding and Aβ positivity in 24 out of the 34 Desikan ROIs after FDR correction (figure 5). The larger number of regions observed may be attributable to increased power due to the increased number of individuals in the Aβ+ group, therefore decreasing the chance of type II errors (i.e., if flortaucipir binding really is elevated in these additional frontal and superior parietal regions in Aβ+ individuals, our previous sample size was too small to detect this meaningful difference). Another possibility is that the additional regional associations that appear could be due to tracer-related noise (Baker et al., 2019).

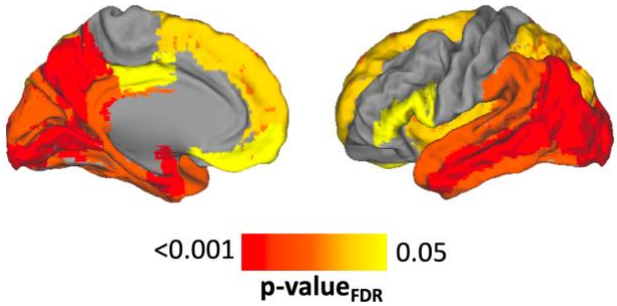

Figure 5: Regions with elevated flortaucipir binding in individuals classified as Aβ+ with precuneus cut off value of 1.489. FDR-corrected p-values of significant regions are projected onto a brain template.

CSF p-tau, flortaucipir, and cortical Aβ. It has been postulated that elevated CSF p-tau in preclinical and early stages of AD may originate from truncated fragments of phosphorylated tau released from neurons in response to cortical Aβ pathology [113]. We found that Aβ+ individuals had higher levels of p-tau than Aβ - individuals (table 1B), and it would be of interest to see if global Aβ mediates or partially mediates the relationship with CSF p-tau and flortaucipir binding in future cross-sectional and longitudinal studies. This could provide further insight into the Aβ cascade hypothesis, as well as the temporal order of CSF p-tau elevation and the spread of neurofibrillary tangle pathology. It is possible that neurotoxic Aβ oligomers or their subsequent form as Aβ senile plaques are involved in the increased rate of phosphorylated tau fragment release into the interstitial fluid and ultimately the CSF while also being involved in mechanisms that facilitate the assembly of neurofibrillary tangles.

Evaluating advanced Braak regions. It was interesting that subsets of regions in advanced Braak stages IV, V and VI showed elevated flortaucipir binding in the Aβ-positive group in this manuscript. We are not the first group to show elevated flortaucipir binding in the lateral occipital gyrus among cognitively normal individuals [65]. Although macroscopic, widespread neurofibrillary tangle pathology is typically observable in Braak stage V, more subtle

elevations may be occurring even earlier. Dr. Heiko Braak himself recently reported that, when studying individual neocortical pyramidal neurons of individuals with macroscopic pathological patterns matching Braak stages I-IV, there exist rare and isolated AT8-immunopositive (i.e., neurofibrillary tangle positive) pyramidal neurons in regions that were previously thought to be affected primarily in Braak stages V and VI [14]. These unexpected AT8-immunopositive pyramidal neurons were consistently observed in peristriatal regions (which includes the lateral occipital gyrus) and the superior temporal lobe. This finding is in line with another recent study that showed that tau seeding activity (i.e. abnormal tau oligomers) were present in the lateral occipital gyrus and superior temporal lobe in individuals with Braak stage III tangle pathology [97]. Therefore, it is possible that flortaucipir is binding to neurofibrillary tangles in sparse, isolated pyramidal neurons in regions such as the lateral occipital gyrus and the superior temporal lobe even before individuals have widespread cortical tau pathology. Further autoradiographic and immunohistochemical studies would be necessary to clarify the presence of lateral occipital tau pathology during preclinical AD.

Clinical trials. Overall, this thesis provides support for encouraging recruitment and enrollment of cognitively normal individuals who have subthreshold levels of tau pathology in anti-tau clinical trials. It also supports the use of tau-PET imaging to identify and evaluate such individuals. While there are several ongoing clinical trials that aim to target tau pathology in AD dementia and other tauopathies in humans, none of them appear to have been tested on humans with pathological profiles consistent with preclinical AD [114]. One trial is planning to evaluate an anti-tau antibody called ABBV-8E12 in humans with early AD, however [115]. ABBV-8E12 is a humanized variation of anti-tau antibodies that decreased levels of cortical tau pathology and prevented the transmission of tau seeding between neurons in a transgenic mouse model of

preclinical tauopathy [116,117]. In this initial experiment, the mice were continuously injected with an anti-tau antibody as soon as they expressed evidence of tau pathology, and one antibody (HJ8.5) significantly reduced cortical tau pathology and improved associative learning [117]. As ABBV-8E12 is modeled on this effective anti-tau antibody, it would be interesting to see if it could reduce or halt the spreading of abnormal tau in cognitively normal humans who are just beginning to show evidence of tau pathology, and ultimately decrease their long-term risk of AD dementia. Recruiting such individuals with a family history of sporadic AD may enrich the sample due to their elevated risk of developing the disease [74].

To date, no anti-tau therapies have been approved for clinical use. However, most AD clinical trials over the past few decades have focused on Aβ, and clinical trials targeting tau have gained traction more recently [118]. Given the major recent advances in both the field's biological understanding of tau pathology and the novel ability to track its progression *in vivo* with tau-PET imaging, anti-tau therapies appear to be a promising pathway of preventing or mitigating the debilitating symptoms of Alzheimer's disease dementia.

Conclusion

Overall, this thesis shows that [^{18}F]flortaucipir binding is associated with cortical Aβ PET binding, CSF p-tau levels, and cognitive performance, especially delayed memory, in older adults who clinically present as cognitively normal. Its associations with established markers of AD provide evidence that flortaucipir is useful for detecting tau pathology, even at the earliest stages of the disease. Additionally, we showed that subthreshold flortaucipir conveys meaningful information about underlying AD-related pathological changes, even at fairly low levels of tracer binding. If anti-tau therapies are found to be effective in cognitively normal individuals with

subthreshold levels of tau pathology, such as the participants in this study, perhaps Alzheimer's disease can, one day, be eradicated all together.

References

1. Meyer P-F, McSweeney M, Gonneaud J, Villeneuve S. PET amyloid imaging across the Alzheimer's disease spectrum: From disease mechanisms to prevention. Progress in Molecular Biology and Translational Science [online]. Academic Press; 2019. Accessed at: http://www.sciencedirect.com/science/article/pii/S1877117319300791. Accessed July 17, 2019.

2. Sperling RA, Aisen PS, Beckett LA, et al. Toward defining the preclinical stages of Alzheimer's disease: recommendations from the National Institute on Aging-Alzheimer's Association workgroups on diagnostic guidelines for Alzheimer's disease. Alzheimers Dement. 2011;7:280–292.

3. Jack CR, Knopman DS, Jagust WJ, et al. Hypothetical model of dynamic biomarkers of the Alzheimer's pathological cascade. The Lancet Neurology. 2010;9:119–128.

4. Jack CR Jr, Bennett DA, Blennow K, et al. NIA-AA Research Framework: Toward a biological definition of Alzheimer's disease. Alzheimers Dement. 2018;14:535–562.

5. Chirita CN, Congdon EE, Yin H, Kuret J. Triggers of Full-Length Tau Aggregation: A Role for Partially Folded Intermediates. Biochemistry. 2005;44:5862–5872.

6. Koffie RM, Hyman BT, Spires-Jones TL. Alzheimer's disease: synapses gone cold. Mol Neurodegener. 2011;6:63.

7. Weingarten MD, Lockwood AH, Hwo SY, Kirschner MW. A protein factor essential for microtubule assembly. Proc Natl Acad Sci U S A. 1975;72:1858–1862.

8. Iqbal K, Liu F, Gong C-X, Grundke-Iqbal I. Tau in Alzheimer disease and related tauopathies. Curr Alzheimer Res. 2010;7:656–664.

9. Braak E, Braak H, Mandelkow EM. A sequence of cytoskeleton changes related to the formation of neurofibrillary tangles and neuropil threads. Acta Neuropathol. 1994;87:554–567.

10. Wiśniewski HM, Narang HK, Terry RD. Neurofibrillary tangles of paired helical filaments. J Neurol Sci. 1976;27:173–181.

11. Arriagada PV, Growdon JH, Hedley-Whyte ET, Hyman BT. Neurofibrillary tangles but not senile plaques parallel duration and severity of Alzheimer's disease. Neurology. 1992;42:631–639.

12. Braak H. Alzheimer's Disease, Neural Basis of. In: Smelser NJ, Baltes PB, editors. International Encyclopedia of the Social & Behavioral Sciences [online]. Oxford: Pergamon; 2001. p. 425–430. Accessed at: http://www.sciencedirect.com/science/article/pii/B0080430767035695. Accessed June 6, 2019.

13. Mudher A, Colin M, Dujardin S, et al. What is the evidence that tau pathology spreads through prion-like propagation? Acta Neuropathol Commun [online serial]. 2017;5. Accessed at: https://www.ncbi.nlm.nih.gov/pmc/articles/PMC5735872/. Accessed July 11, 2019.

14. Braak H, Del Tredici K. Spreading of Tau Pathology in Sporadic Alzheimer's Disease Along Cortico-cortical Top-Down Connections. Cereb Cortex. 2018;28:3372–3384.

15. Braak H, Braak E. Neuropathological stageing of Alzheimer-related changes. Acta Neuropathol. 1991;82:239–259.

16. Murphy MP, LeVine H. Alzheimer's disease and the amyloid-beta peptide. J Alzheimers Dis. 2010;19:311–323.

17. Bitan G, Kirkitadze MD, Lomakin A, Vollers SS, Benedek GB, Teplow DB. Amyloid beta -protein (Abeta) assembly: Abeta 40 and Abeta 42 oligomerize through distinct pathways. Proc Natl Acad Sci USA. 2003;100:330–335.

18. Demuro A, Mina E, Kayed R, Milton SC, Parker I, Glabe CG. Calcium Dysregulation and Membrane Disruption as a Ubiquitous Neurotoxic Mechanism of Soluble Amyloid Oligomers. J Biol Chem. 2005;280:17294–17300.

19. Sengupta U, Nilson AN, Kayed R. The Role of Amyloid-β Oligomers in Toxicity, Propagation, and Immunotherapy. EBioMedicine. 2016;6:42–49.

20. Thal DR. Clearance of Amyloid β-Protein and its role in the Spreading of Alzheimer's disease Pathology. Front Aging Neurosci [online serial]. 2015;7. Accessed at: https://www.frontiersin.org/articles/10.3389/fnagi.2015.00025/full. Accessed July 9, 2019.

21. Thal DR, Rüb U, Orantes M, Braak H. Phases of A beta-deposition in the human brain and its relevance for the development of AD. Neurology. 2002;58:1791–1800.

22. Buckner RL, Snyder AZ, Shannon BJ, et al. Molecular, structural, and functional characterization of Alzheimer's disease: evidence for a relationship between default activity, amyloid, and memory. J Neurosci. 2005;25:7709–7717.

23. Gonneaud J, Arenaza-Urquijo EM, Mézenge F, et al. Increased florbetapir binding in the temporal neocortex from age 20 to 60 years. Neurology. 2017;89:2438–2446.

24. Palmqvist S, Schöll M, Strandberg O, et al. Earliest accumulation of β-amyloid occurs within the default-mode network and concurrently affects brain connectivity. Nature Communications. 2017;8:1214.

25. Villeneuve S, Rabinovici GD, Cohn-Sheehy BI, et al. Existing Pittsburgh Compound-B positron emission tomography thresholds are too high: statistical and pathological evaluation. Brain. 2015;138:2020–2033.

26. Wagner AD, Shannon BJ, Kahn I, Buckner RL. Parietal lobe contributions to episodic memory retrieval. Trends Cogn Sci (Regul Ed). 2005;9:445–453.

27. Jones DT, Knopman DS, Gunter JL, et al. Cascading network failure across the Alzheimer's disease spectrum. Brain. 2016;139:547–562.

28. Jagust W. Imaging the evolution and pathophysiology of Alzheimer disease. Nat Rev Neurosci. 2018;19:687–700.

29. Sepulcre J, Schultz AP, Sabuncu M, et al. In Vivo Tau, Amyloid, and Gray Matter Profiles in the Aging Brain. J Neurosci. 2016;36:7364–7374.

30. Villeneuve S, Wirth M, La Joie R. Are AD-Typical Regions the Convergence Point of Multiple Pathologies? Front Aging Neurosci. 2015;7:42.

31. Barthélemy NR, Mallipeddi N, Moiseyev P, Sato C, Bateman RJ. Tau Phosphorylation Rates Measured by Mass Spectrometry Differ in the Intracellular Brain vs. Extracellular Cerebrospinal Fluid Compartments and Are Differentially Affected by Alzheimer's Disease. Front Aging Neurosci [online serial]. 2019;11. Accessed at: https://www.frontiersin.org/articles/10.3389/fnagi.2019.00121/full. Accessed July 24, 2019.

32. Blennow K, Hampel H. CSF markers for incipient Alzheimer's disease. Lancet Neurol. 2003;2:605–613.

33. Skillbäck T, Rosén C, Asztely F, Mattsson N, Blennow K, Zetterberg H. Diagnostic performance of cerebrospinal fluid total tau and phosphorylated tau in Creutzfeldt-Jakob disease: results from the Swedish Mortality Registry. JAMA Neurol. 2014;71:476–483.

34. Mattsson Niklas, Schöll Michael, Strandberg Olof, et al. 18F-AV-1451 and CSF T-tau and P-tau as biomarkers in Alzheimer's disease. EMBO Mol Med. 2017;9:1212–1223.

35. Salmon DP, Bondi MW. Neuropsychological Assessment of Dementia. Annu Rev Psychol. 2009;60:257–282.

36. Weintraub S, Wicklund AH, Salmon DP. The neuropsychological profile of Alzheimer disease. Cold Spring Harb Perspect Med. 2012;2:a006171.

37. Dubois B, Albert ML. Amnestic MCI or prodromal Alzheimer's disease? Lancet Neurol. 2004;3:246–248.

38. Salmon DP. Disorders of memory in Alzheimer's disease. Handbook of neuropsychology: Memory and its disorders, Vol 2, 2nd ed. Amsterdam, Netherlands: Elsevier Science Publishers B.V.; 2000. p. 155–195.

39. Ho JK, Nation DA, Alzheimer's Disease Neuroimaging Initiative. Neuropsychological Profiles and Trajectories in Preclinical Alzheimer's Disease. J Int Neuropsychol Soc. 2018;24:693–702.

40. Duke Han S, Nguyen CP, Stricker NH, Nation DA. Detectable Neuropsychological Differences in Early Preclinical Alzheimer's Disease: A Meta-Analysis. Neuropsychol Rev. 2017;27:305–325.

41. Rogalski E, Sridhar J, Rader B, et al. Aphasic variant of Alzheimer disease: Clinical, anatomic, and genetic features. Neurology. 2016;87:1337–1343.

42. Weintraub S, Carrillo MC, Farias ST, et al. Measuring cognition and function in the preclinical stage of Alzheimer's disease. Alzheimers Dement (N Y). 2018;4:64–75.

43. Konishi K, Joober R, Poirier J, et al. Healthy versus Entorhinal Cortical Atrophy Identification in Asymptomatic APOE4 Carriers at Risk for Alzheimer's Disease. J Alzheimers Dis. 2018;61:1493–1507.

44. Zhang W, Arteaga J, Cashion DK, et al. A highly selective and specific PET tracer for imaging of tau pathologies. J Alzheimers Dis. 2012;31:601–612.

45. Braak H, Alafuzoff I, Arzberger T, Kretzschmar H, Del Tredici K. Staging of Alzheimer disease-associated neurofibrillary pathology using paraffin sections and immunocytochemistry. Acta Neuropathol. 2006;112:389–404.

46. Brettschneider J, Del Tredici K, Lee VM-Y, Trojanowski JQ. Spreading of pathology in neurodegenerative diseases: a focus on human studies. Nat Rev Neurosci. 2015;16:109–120.

47. Iaccarino L, Tammewar G, Ayakta N, et al. Local and distant relationships between amyloid, tau and neurodegeneration in Alzheimer's Disease. Neuroimage Clin. 2018;17:452–464.

48. Musiek ES, Holtzman DM. Three dimensions of the amyloid hypothesis: time, space and "wingmen." Nat Neurosci. 2015;18:800–806.

49. Schöll M, Lockhart SN, Schonhaut DR, et al. PET Imaging of Tau Deposition in the Aging Human Brain. Neuron. 2016;89:971–982.

50. Vemuri P, Lowe VJ, Knopman DS, et al. Tau-PET uptake: Regional variation in average SUVR and impact of amyloid deposition. Alzheimers Dement (Amst). 2016;6:21–30.

51. Hall B, Mak E, Cervenka S, Aigbirhio FI, Rowe JB, O'Brien JT. In vivo tau PET imaging in dementia: Pathophysiology, radiotracer quantification, and a systematic review of clinical findings. Ageing Res Rev. 2017;36:50–63.

52. Ossenkoppele R, Rabinovici GD, Smith R, et al. Discriminative Accuracy of [18F]flortaucipir Positron Emission Tomography for Alzheimer Disease vs Other Neurodegenerative Disorders. JAMA. 2018;320:1151–1162.

53. Okamura N, Harada R, Ishiki A, Kikuchi A, Nakamura T, Kudo Y. The development and validation of tau PET tracers: current status and future directions. Clin Transl Imaging. 2018;6:305–316.

54. Lowe VJ, Curran G, Fang P, et al. An autoradiographic evaluation of AV-1451 Tau PET in dementia. Acta Neuropathol Commun [online serial]. 2016;4. Accessed at: https://www.ncbi.nlm.nih.gov/pmc/articles/PMC4906968/. Accessed December 20, 2018.

55. Lemoine L, Leuzy A, Chiotis K, Rodriguez-Vieitez E, Nordberg A. Tau positron emission tomography imaging in tauopathies: The added hurdle of off-target binding. Alzheimer's & Dementia: Diagnosis, Assessment & Disease Monitoring. 2018;10:232–236.

56. Marquié M, Normandin MD, Vanderburg CR, et al. Validating novel tau positron emission tomography tracer [F-18]-AV-1451 (T807) on postmortem brain tissue. Annals of Neurology. 2015;78:787–800.

57. Baker SL, Maass A, Jagust WJ. Considerations and code for partial volume correcting [18F]-AV-1451 tau PET data. Data Brief. 2017;15:648–657.

58. Cho H, Choi JY, Hwang MS, et al. In vivo cortical spreading pattern of tau and amyloid in the Alzheimer disease spectrum. Ann Neurol. 2016;80:247–258.

59. Kinahan PE, Fletcher JW. PET/CT Standardized Uptake Values (SUVs) in Clinical Practice and Assessing Response to Therapy. Semin Ultrasound CT MR. 2010;31:496–505.

60. Thie JA. Understanding the Standardized Uptake Value, Its Methods, and Implications for Usage. J Nucl Med. 2004;45:1431–1434.

61. Charney DS, Nestler EJ, Sklar PS, Buxbaum JD. Charney & Nestler's Neurobiology of Mental Illness. Oxford University Press; 2017.

62. Catafau AM, Bullich S, Seibyl JP, et al. Cerebellar Amyloid-β Plaques: How Frequent Are They, and Do They Influence 18F-Florbetaben SUV Ratios? J Nucl Med. 2016;57:1740–1745.

63. Fleisher AS, Chen K, Liu X, et al. Using Positron Emission Tomography and Florbetapir F 18 to Image Cortical Amyloid in Patients With Mild Cognitive Impairment or Dementia Due to Alzheimer Disease. Arch Neurol. 2011;68:1404–1411.

64. Maass A, Lockhart SN, Harrison TM, et al. Entorhinal Tau Pathology, Episodic Memory Decline, and Neurodegeneration in Aging. J Neurosci. 2018;38:530–543.

65. Mishra S, Gordon BA, Su Y, et al. AV-1451 PET imaging of tau pathology in preclinical Alzheimer disease: Defining a summary measure. Neuroimage. 2017;161:171–178.

66. Chhatwal JP, Schultz AP, Marshall GA, et al. Temporal T807 binding correlates with CSF tau and phospho-tau in normal elderly. Neurology. 2016;87:920–926.

67. Gordon BA, Friedrichsen K, Brier M, et al. The relationship between cerebrospinal fluid markers of Alzheimer pathology and positron emission tomography tau imaging. Brain. 2016;139:2249–2260.

68. Jack CR Jr, Wiste HJ, Weigand SD, et al. Defining imaging biomarker cut points for brain aging and Alzheimer's disease. Alzheimers Dement. 2017;13:205–216.

69. Maass A, Landau S, Baker SL, et al. Comparison of multiple tau-PET measures as biomarkers in aging and Alzheimer's disease. Neuroimage. 2017;157:448–463.

70. Nai Y-H, Shidahara M, Seki C, Watabe H. Biomathematical screening of amyloid radiotracers with clinical usefulness index. Alzheimers Dement (N Y). 2017;3:542–552.

71. Mormino EC, Kluth JT, Madison CM, et al. Episodic memory loss is related to hippocampal-mediated beta-amyloid deposition in elderly subjects. Brain. 2009;132:1310–1323.

72. Bassett SS, Yousem DM, Cristinzio C, et al. Familial risk for Alzheimer's disease alters fMRI activation patterns. Brain. 2006;129:1229–1239.

73. Cupples LA, Farrer LA, Sadovnick AD, Relkin N, Whitehouse P, Green RC. Estimating risk curves for first-degree relatives of patients with Alzheimer's disease: the REVEAL study. Genet Med. 2004;6:192–196.

74. Cannon-Albright LA, Foster NL, Schliep K, et al. Relative risk for Alzheimer disease based on complete family history. Neurology. 2019;92:e1745–e1753.

75. Poirier J, Davignon J, Bouthillier D, Kogan S, Bertrand P, Gauthier S. Apolipoprotein E polymorphism and Alzheimer's disease. Lancet. 1993;342:697–699.

76. Sando SB, Melquist S, Cannon A, et al. APOE ε4 lowers age at onset and is a high risk factor for Alzheimer's disease; A case control study from central Norway. BMC Neurology. 2008;8:9.

77. Gatz M, Reynolds CA, Fratiglioni L, et al. Role of genes and environments for explaining Alzheimer disease. Arch Gen Psychiatry. 2006;63:168–174.

78. Ridge PG, Hoyt KB, Boehme K, et al. Assessment of the genetic variance of late-onset Alzheimer's disease. Neurobiology of Aging. 2016;41:200.e13-200.e20.

79. de Bruijn RFAG, Bos MJ, Portegies MLP, et al. The potential for prevention of dementia across two decades: the prospective, population-based Rotterdam Study. BMC Med. 2015;13:132.

80. Schöll M, Maass A, Mattsson N, et al. Biomarkers for tau pathology. Molecular and Cellular Neuroscience. 2019;97:18–33.

81. Amieva H, Le Goff M, Millet X, et al. Prodromal Alzheimer's disease: successive emergence of the clinical symptoms. Ann Neurol. 2008;64:492–498.

82. Ohm TG, Müller H, Braak H, Bohl J. Close-meshed prevalence rates of different stages as a tool to uncover the rate of Alzheimer's disease-related neurofibrillary changes. Neuroscience. 1995;64:209–217.

83. Ariza M, Kolb HC, Moechars D, Rombouts F, Andrés JI. Tau Positron Emission Tomography (PET) Imaging: Past, Present, and Future. J Med Chem. 2015;58:4365–4382.

84. Saint-Aubert L, Lemoine L, Chiotis K, Leuzy A, Rodriguez-Vieitez E, Nordberg A. Tau PET imaging: present and future directions. Molecular Neurodegeneration. 2017;12:19.

85. Schwarz AJ, Yu P, Miller BB, et al. Regional profiles of the candidate tau PET ligand 18F-AV-1451 recapitulate key features of Braak histopathological stages. Brain. 2016;139:1539–1550.

86. Lowe VJ, Wiste HJ, Senjem ML, et al. Widespread brain tau and its association with ageing, Braak stage and Alzheimer's dementia. Brain. 2018;141:271–287.

87. Hebert LE, Weuve J, Scherr PA, Evans DA. Alzheimer disease in the United States (2010-2050) estimated using the 2010 census. Neurology. 2013;80:1778–1783.

88. Breitner JCS, Poirier J, Etienne PE, Leoutsakos JM. Rationale and structure for a new center for studies on prevention of Alzheimer's disease (STOP-AD). The Journal of Prevention of Alzheimer's Disease. 2016;3:36–42.

89. Reuter M, Rosas H D, Fischl B. Highly Accurate Inverse Consistent Registration: A Robust Approach. Neuroimage. 2010;53:1181–1196.

90. Desikan RS, Ségonne F, Fischl B, et al. An automated labeling system for subdividing the human cerebral cortex on MRI scans into gyral based regions of interest. Neuroimage. 2006;31:968–980.

91. Villeneuve S, Vogel JW, Gonneaud J, et al. Proximity to Parental Symptom Onset and Amyloid-β Burden in Sporadic Alzheimer Disease. JAMA Neurol [online serial]. Epub 2018 Feb 26. Accessed at: http://dx.doi.org/10.1001/jamaneurol.2017.5135.

92. Randolph C, Tierney MC, Mohr E, Chase TN. The Repeatable Battery for the Assessment of Neuropsychological Status (RBANS): preliminary clinical validity. J Clin Exp Neuropsychol. 1998;20:310–319.

93. Benjamini Y, Hochberg Y. Controlling the False Discovery Rate: A Practical and Powerful Approach to Multiple Testing. Journal of the Royal Statistical Society Series B (Methodological). 1995;57:289–300.

94. Winkler AM, Ridgway GR, Webster MA, Smith SM, Nichols TE. Permutation inference for the general linear model. Neuroimage. 2014;92:381–397.

95. Crary JF, Trojanowski JQ, Schneider JA, et al. Primary age-related tauopathy (PART): a common pathology associated with human aging. Acta Neuropathol. 2014;128:755–766.

96. Braak H, Thal DR, Ghebremedhin E, Del Tredici K. Stages of the pathologic process in Alzheimer disease: age categories from 1 to 100 years. J Neuropathol Exp Neurol. 2011;70:960–969.

97. Kaufman SK, Del Tredici K, Thomas TL, Braak H, Diamond MI. Tau seeding activity begins in the transentorhinal/entorhinal regions and anticipates phospho-tau pathology in Alzheimer's disease and PART. Acta Neuropathol. 2018;136:57–67.

98. Bateman RJ, Xiong C, Benzinger TLS, et al. Clinical and biomarker changes in dominantly inherited Alzheimer's disease. N Engl J Med. 2012;367:795–804.

99. Mormino EC, Brandel MG, Madison CM, et al. Not quite PIB-positive, not quite PIB-negative: slight PIB elevations in elderly normal control subjects are biologically relevant. Neuroimage. 2012;59:1152–1160.

100. Bischof GN, Jacobs HIL. Subthreshold amyloid and its biological and clinical meaning: Long way ahead. Neurology. 2019;93:72–79.

101. Smith R, Wibom M, Pawlik D, Englund E, Hansson O. Correlation of In Vivo [18F]Flortaucipir With Postmortem Alzheimer Disease Tau Pathology. JAMA Neurol. Epub 2018 Dec 3.

102. Marquié M, Siao Tick Chong M, Antón-Fernández A, et al. [F-18]-AV-1451 binding correlates with postmortem neurofibrillary tangle Braak staging. Acta Neuropathol. 2017;134:619–628.

103. Schöll M, Ossenkoppele R, Strandberg O, et al. Distinct 18F-AV-1451 tau PET retention patterns in early- and late-onset Alzheimer's disease. Brain. 2017;140:2286–2294.

104. Blennow K, Hampel H, Weiner M, Zetterberg H. Cerebrospinal fluid and plasma biomarkers in Alzheimer disease. Nat Rev Neurol. 2010;6:131–144.

105. La Joie R, Bejanin A, Fagan AM, et al. Associations between [18F]AV1451 tau PET and CSF measures of tau pathology in a clinical sample. Neurology. 2018;90:e282–e290.

106. Leal SL, Lockhart SN, Maass A, Bell RK, Jagust WJ. Subthreshold Amyloid Predicts Tau Deposition in Aging. J Neurosci. 2018;38:4482–4489.

107. Gao Y-L, Wang N, Sun F-R, Cao X-P, Zhang W, Yu J-T. Tau in neurodegenerative disease. Ann Transl Med [online serial]. 2018;6. Accessed at: https://www.ncbi.nlm.nih.gov/pmc/articles/PMC5994507/. Accessed August 14, 2019.

108. Iqbal K, Liu F, Gong C-X. Tau and neurodegenerative disease: the story so far. Nature Reviews Neurology. 2016;12:15–27.

109. Fratiglioni L, Wang H-X. Brain reserve hypothesis in dementia. J Alzheimers Dis. 2007;12:11–22.

110. Sperling RA, Mormino EC, Schultz AP, et al. The impact of amyloid-beta and tau on prospective cognitive decline in older individuals. Annals of Neurology. 2019;85:181–193.

111. Aschenbrenner AJ, Gordon BA, Benzinger TLS, Morris JC, Hassenstab JJ. Influence of tau PET, amyloid PET, and hippocampal volume on cognition in Alzheimer disease. Neurology. 2018;91:e859–e866.

112. Mattsson N, Palmqvist S, Stomrud E, Vogel J, Hansson O. Staging β-Amyloid Pathology With Amyloid Positron Emission Tomography. JAMA Neurol [online serial]. Epub 2019 Jul 17. Accessed at: https://jamanetwork.com/journals/jamaneurology/fullarticle/2738356. Accessed July 24, 2019.

113. Sato C, Barthélemy NR, Mawuenyega KG, et al. Tau Kinetics in Neurons and the Human Central Nervous System. Neuron. 2018;97:1284-1298.e7.

114. Cummings J, Blennow K, Johnson K, et al. Anti-Tau Trials for Alzheimer's Disease: A Report from the EU/US/CTAD Task Force. J Prev Alzheimers Dis. 2019;6:157–163.

115. West T, Hu Y, Verghese PB, et al. Preclinical and Clinical Development of ABBV-8E12, a Humanized Anti-Tau Antibody, for Treatment of Alzheimer's Disease and Other Tauopathies. J Prev Alzheimers Dis. 2017;4:236–241.

116. Ising C, Gallardo G, Leyns CEG, et al. AAV-mediated expression of anti-tau scFvs decreases tau accumulation in a mouse model of tauopathy. J Exp Med. 2017;214:1227–1238.

117. Yanamandra K, Kfoury N, Jiang H, et al. Anti-tau antibodies that block tau aggregate seeding in vitro markedly decrease pathology and improve cognition in vivo. Neuron. 2013;80:402–414.

118. Medina M. An Overview on the Clinical Development of Tau-Based Therapeutics. Int J Mol Sci [online serial]. 2018;19. Accessed at: https://www.ncbi.nlm.nih.gov/pmc/articles/PMC5979300/. Accessed July 11, 2019.